AIS Ranging and Positioning - concept and signal design

GA5.3/5.4 intermediate project report

Issue: 1.0

Issue Status: Approved

Issue Date: 24/10/2019

	Name	Partner	Signature
Provided	Krzysztof Bronk	NIT	
Review	Stefan Gewies	DLR	
Approval	Stefan Gewies	DLR	

Document Information

Project Title	R-Mode Baltic
Work Package No.	GA 5.3/5.4
Document Title	AIS Ranging and Positioning - concept and signal design
Description	The major topic of the document is the AIS system and its possible utilization for the purpose of the future R-Mode Baltic solution
Date	24.10.2021
Lead Author	NIT
Lead Author's Contact Information	National Institute of Telecommunications Wireless Systems and Networks Department Telephone: (+48) 58 341 71 21 E-mail: K.Bronk@itl.waw.pl
Contributing Author(s)	Krzysztof Bronk, Magdalena Januszewska, Patryk Koncicki, Rafał Niski, Błażej Wereszko
Approval	Yes

Track Changes

Issue	Date	Pages	Change	Author, Company
1.0	27/03/2019	69	Draft	NIT

This report was created within the framework of the **R-Mode Baltic** project, which aims to develop and demonstrate a new maritime backup system for Position, Navigation and Time (PNT) purposes based on R-Mode technology. Within the project life time of three years the project consortium develops solutions for R-Mode transmitter and receiver prototypes, for independent time synchronisations of broadcasting stations and for a testbed concept and its deployment. The dissemination of R-Mode technology is supported by work in international standardisation bodies. The world's first operational testbed for a transnational R-Mode system will be completed by the project in 2020.

The R-Mode Baltic project is co-financed by the European Regional Development Fund within the Interreg Baltic Sea Region Programme.

This report is available for download on the project website https://www.r-mode-baltic.eu/.

Contents

List of Tables

List of Figures

Abbreviations

AIS	Automatic Identification System
AWGN	Additive White Gaussian Noise
BER	Bit Error Rate
BLER	Block Error Rate
CRC	Cyclic Redundancy Check
GMSK	Gaussian Minimum Shift Keying
GNSS	Global Navigation Satellite System
GPS	Global Positioning System
LPF	Low-pass filter
NRZI	Non Return to Zero Inverted
PNT	Position, Navigation and Time
R-Mode	Ranging Mode
SDR	Software Defined Radio
TOA	Time of Arrival
USRP	Universal Software Radio Peripheral
VDES	VHF Data Exchange System

1 Introduction

The following report summarises the activities of the National Institute of Telecommunications in the R-Mode's GAs 5.3 and 5.4. The major topic of the document is the AIS system and its possible utilization for the purpose of the future R-Mode Baltic solution.

The report is comprised of eight chapters (including this introduction).

The second chapter introduces the concept of the AIS Message 26 utilization for the R-Mode synchronization codes transmission. Most notably it presents the synchronization codes selected for this purpose and discusses their correlation properties.

The next, third, chapter is dedicated to the issue of distance determination accuracy in the R-Mode system. It discusses the influence of the AIS message 26 length (1,2 or 5 slots) on the distance accuracy.

The fourth chapter provides a detailed description of the software implementation of the AIS system (transmitter, channel, receiver) as well as the hardware platform that is being prepared for the upcoming measurement campaigns. In both cases, the correctness of these implementations was confirmed by simulations the results of which are also included in the chapter.

In the fifth chapter, authors introduced the methodology to be used during the R-Mode measurement scheduled to take place at the Baltic Sea in the spring 2019. At this stage, a close cooperation with the Maritime Office in Gdynia (a partner in the R-Mode project) was established.

Sixth chapter presents the software localization simulator which allows to analyse the performance of positioning algorithms, particularly the TDOA, in the presence of various sources of errors that may affect the efficiency of such algorithms. In the chapter, the general concept of the simulator is outlined, alongside some initial simulation results.

The seventh chapter is dedicated to the analysis of the phenomena occurring in the troposphere and the ways of their mathematical analysis. The major input for the chapter were recommendations issued by the ITU-R.

In the last chapter, some final remarks are included, mostly regarding the future tasks to be carried out by the National Institute of Telecommunication in the R-Mode project.

2 The AIS signal's usage concept

2.1 The AIS ranging

One of the basic R-Mode project assumptions is the usage of the Automatic Identification System's (AIS) standard messages for ranging measurements. The project requirements indicate the AIS Message 26 should be used [2-1]. The multiple slot binary Message 26 is primarily intended for scheduled binary data transmissions by applying either the SOTDMA or ITDMA access schemes. This multiple slot binary message can contain up to 1 004 data bits (using 5 slots) depending on the coding method used for the content, and the destination indication of broadcast or addressed. The table 2-1 presents the Message 26 structure tailored to the project purposes [2-2].

Table 2-1: AIS Message 26 structure [2-2]

Parameter	Number of bits	Description
Message ID	6	Identifier for Message 26; always 26
Repeat indicator	2	Used by the repeater to indicate how many times a message has been repeated; default = 0
Source ID	30	MMSI number of source station
Destination indicator	1	0 = Broadcast (no Destination ID field used)
Binary data flag	1	1 = binary data coded as defined by using the 16-bit Application identifier
Binary data	104	Application identifier - 16 bits
		Application binary data - 88 bits
Binary data added by 2nd slot	224	Allows for 32 bits of bit-stuffing
Binary data added by 3rd slot	224	Allows for 32 bits of bit-stuffing
Binary data added by 4th slot	224	Allows for 32 bits of bit-stuffing
Binary data added by 5th slot	224	Allows for 32 bits of bit-stuffing
Spare	4	Needed for byte alignment
Communication state selector flag	1	0 = SOTDMA communication state follows 1 = ITDMA communication state follows
Communication state	19	SOTDMA communication state if communication state selector flag is set to 0, or ITDMA communication state if communication state selector flag is set to 1
Maximum number of bits	Maximum 1 064	

The table 2-2 contains the maximum number of binary data-bits for settings of destination indicator and coding method flags, such that the message does not exceed the indicated number of slots.

Table 2-2: Maximum number of AIS Message 26 data bits [2-2]

Destination indicator	Binary data flag	Binary data (maximum bits)				
		1-slot	2-slot	3-slot	4-slot	5-slot
0	1	88	312	536	760	984

The assumption of the R-Mode project is to send the synchronization code within the AIS Message 26 and to use the TOA method in order to determine the distance between the terminal (ship) and the base station (shore). At the current stage of the project, it is assumed to use different lengths of the synchronization code and different forms (lengths) of the Message 26. It is known that the accuracy of determining this distance depends on the synchronization code length and it is recommended that it should be as long as possible. On the other hand, the resources of AIS system are limited and their use for purposes other than maritime safety should be kept to a minimum. Therefore, in the further project stages, the measurements will be conducted to allow selecting the appropriate target form of the R-Mode navigation message, which will depend on the established, maximum acceptable AIS system load.

Let us consider three cases of different lengths of the R-Mode navigation message: respectively 1, 2 and 5 slots. Assuming that a few bits (up to 8) have to be allocated to information about the base station status (and some other information not yet specified), then the synchronization code will have a length of respectively about 80, 300 and 970 bits.

Due to the NRZI coding scheme defined in the AIS system [2-2] as well as synchronization mechanisms and the forms of start and end flags defining the beginning and end of the frame, the synchronization code form can't be arbitrary. The main limitation is the bit stuffing mechanism, which applies to all bits between the start and end flags. On the transmitting side, if five (5) consecutive ones (1) are found in the output bit stream, a zero (0) should be inserted after them and on the receiving side, the first zero (0) after five (5) consecutive ones (1) should be removed. Therefore, the synchronization code must be selected so that it is not "supplemented" by additional bits that may adversely affect its correlation properties, and the code length fits to different lengths of R-Mode navigation messages. If the code fulfils the bit stuffing criteria and no additional bits are inserted, the length of that synchronization code can potentially be bigger than the normal AIS message limits and utilise the bits reserved for the bit stuffing (32 bits in each slot). Therefore the maximum length of the synchronization code for the 5 slots message is up to 1100 bits (1064+4x32).

2.2 The synchronization codes

When searching for the appropriate synchronization code, it was decided to use the Gold's sequences and the long uplink scrambling code generator defined for the UMTS system [2-3]. The code generator is constructed of two generator polynomials of degree 25: $X^{25}+X^3+1$ and $X^{25}+X^3+X^2+X+1$. The two output scrambling sequences are constructed from modulo 2 sum of two binary sequences generated by those polynomials. The resulting sequences have bipolar values (+1 and -1) and constitute segments of a set of

the Gold sequences. The construction of the UMTS uplink scrambling code generator is shown in figure 2-1. Nominally the length of the scrambling code is 38400 chips, so it can be easily shortened.

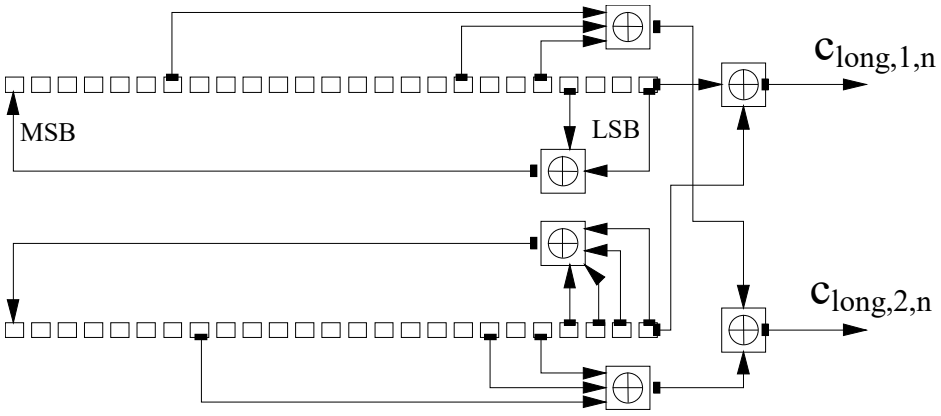

Figure 2-1: Configuration of the UMTS uplink scrambling sequence generator [2-3]

Finally, the complex-valued long scrambling sequence is defined as [2-3]:

$$C_n(i) = c_{long,1,n}(i) \cdot \left[1 + j \cdot (-1)^i \cdot c_{long,2,n}\left(2\left\lfloor {}^{i}/_{2} \right\rfloor\right)\right] \quad (2\text{-}1)$$

where:

i is the number of consecutive bits of the sequence,

n is the 24 bit binary representation of the scrambling sequence number,

⌊ ⌋ denotes rounding to the nearest lower integer.

In order to determine the maximum length of Gold's code obtained using UMTS generator, which will not require the insertion of additional bits by the AIS bit stuffing mechanism, the simulation tests were carried out for all 2^{24} (over 16.7 million) possible combinations of initial states of the generator (scrambling sequence number).

As it was mentioned, the sequence generated by this method is originally bipolar, so in the first step, a code was searched that would correspond to the binary sequence coded by the NRZI encoder. In that case the longest code that meets the bit stuffing criteria (there is no five consecutive “+1” and no five consecutive “-1” bit values) has a length of 463 bits and there is only one such code (initial state 8 889 334) and it is the imaginary part of the generated Gold code.

In the second step the bipolar code sequence has been converted to the binary form (bipolar “1” denotes binary “0” and bipolar “-1” denotes binary “1”). As a result, it was established that the longest code that meets the bit stuffing criteria (there is no five consecutive “1”) has a length of 885 bits and there are 2 such codes (initial states 4 731 302 and 12 862 768) and they are also the imaginary part of the generated Gold code.

In the third step the bipolar code sequence has been converted to the negative binary form (bipolar “1” denotes binary “1” and bipolar “-1” denotes binary “0”). As a result, it was established that the longest code that meets the bit stuffing criteria (there is no five consecutive “1”) has a length of 968 bits and there is only one such code (initial state 702 948) and it is also the imaginary part of the generated Gold code.

Since the code obtained in the third stage is the longest one, it was decided to use that code in further considerations.

The selected synchronization code with initial state 702 948 and length 968 bits is:

0,0,0,0,0,1,1,0,0,1,1,0,1,0,1,1,0,0,0,0,0,0,0,1,1,1,1,0,1,1,0,0,1,0,1,1,0,1,1,1,0,1,1,0,0,0,1,1,1,
1,0,0,1,1,1,0,1,0,0,0,0,0,0,0,0,1,0,0,1,0,0,1,1,0,0,1,0,1,1,0,0,0,1,1,0,0,0,1,0,1,0,0,1,0,1,0,1,1,
0,0,1,1,1,0,1,1,0,0,1,1,0,1,0,0,1,1,1,1,1,0,1,1,0,1,1,1,1,1,0,0,1,1,0,0,0,0,1,0,0,0,0,0,0,1,1,1,1,0,0,
1,0,1,1,0,1,1,0,0,0,1,0,0,0,1,0,1,0,1,0,0,0,1,0,1,0,0,0,1,1,0,1,1,0,0,1,0,0,1,1,0,1,1,1,0,0,0,1,0,
0,1,0,0,0,1,0,0,1,1,0,0,0,0,0,0,0,0,1,1,0,1,0,0,0,1,0,1,1,0,1,0,0,1,0,0,1,1,1,0,1,0,0,0,0,0,0,0,0,1,
1,0,0,1,1,0,0,1,0,1,1,1,0,1,1,0,0,1,0,1,1,0,0,1,0,0,1,1,1,0,1,0,0,1,0,1,0,1,0,0,1,1,0,1,1,0,0,0,0,
0,1,1,0,0,1,0,0,1,1,0,1,0,1,0,1,0,1,0,0,1,0,1,0,1,0,0,0,1,0,0,1,0,0,1,0,1,0,0,0,0,1,0,1,0,1,0,1,1,
1,1,0,1,0,0,1,0,0,0,0,0,1,1,0,0,1,0,1,0,0,0,1,0,0,0,0,0,0,0,0,0,1,0,1,0,1,1,0,1,1,0,0,1,0,1,0,0,0,0,
1,1,0,0,0,1,0,1,0,1,0,1,0,0,0,1,1,1,0,0,0,0,1,1,0,1,1,0,1,1,1,0,0,0,0,1,0,0,0,1,1,0,0,1,1,0,0,1,0,
0,0,1,0,0,1,1,0,1,1,0,0,0,1,1,1,0,1,0,0,1,1,1,0,0,0,0,1,1,1,0,0,1,1,0,1,1,0,0,0,0,0,0,1,1,1,0,0,1,
0,1,1,1,0,0,1,0,1,1,1,0,0,0,1,0,1,1,1,1,0,1,0,1,1,0,1,0,1,0,1,1,1,0,0,1,0,0,1,0,1,1,1,1,0,1,1,1,0,
0,1,1,1,1,0,0,0,0,1,0,0,1,0,0,1,0,1,0,1,1,1,1,0,0,0,1,1,1,0,0,0,0,0,0,0,0,0,0,0,0,0,1,1,0,0,1,0,
1,0,1,0,1,1,0,0,0,0,1,1,1,1,0,1,0,0,0,1,0,1,1,0,0,1,0,0,1,0,0,0,0,0,0,0,0,0,0,1,1,1,0,0,0,1,1,1,0,
0,0,0,1,0,1,0,1,1,1,0,0,1,0,0,0,1,1,1,0,1,1,0,0,1,1,0,1,0,0,1,1,0,0,1,0,0,0,1,0,1,1,0,0,0,0,1,0,1,
0,1,0,1,1,1,1,1,0,1,0,1,1,0,0,0,0,1,1,1,0,0,1,0,1,0,1,1,0,1,0,0,1,0,1,0,1,0,1,0,1,0,1,1,1,0,0,1,1,1,
0,1,0,0,0,0,1,1,0,1,0,0,1,1,1,0,0,1,1,1,1,0,1,1,0,0,0,0,0,1,1,1,0,1,0,0,1,1,0,1,1,1,1,1,0,1,1,1,0,0,
1,0,0,1,1,0,1,0,1,1,0,1,0,0,1,1,0,1,0,1,1,0,1,1,0,1,0,1,1,1,0,1,1,1,1,0,1,0,1,0,0,0,1,0,1,0,1,0,1,
1,0,0,0,1,1,0,0,1,1,0,0,0,1,0,0,1,1,1,0,1,0,1,1,0,1,1,1,0,0,1,1,0,1,0,1,0,1,0,1,1,0,0,1,0,0,0,1,1,
0,0,1,0,1,0,0,0,1,1,0,0,1,1,1,0,0,0,1,1,1,0,1,0,0,0,0,1,0,0,1,1,1,0,0,1,1,1,1,0,0,1,1,0,0,0,0,0,0,
0,1,1,1,1,0,0,0,0,0,1,0,0,0,1,0,1,1,1,0,1,1,1,1,0,1,0,1,1,0,1,0,1,1,1,1,1

In the next stage the selected synchronization code was NRZI coded and its autocorrelation function has been determined and compared with the autocorrelation function before coding. Both autocorrelation functions are presented in figure 2-2.

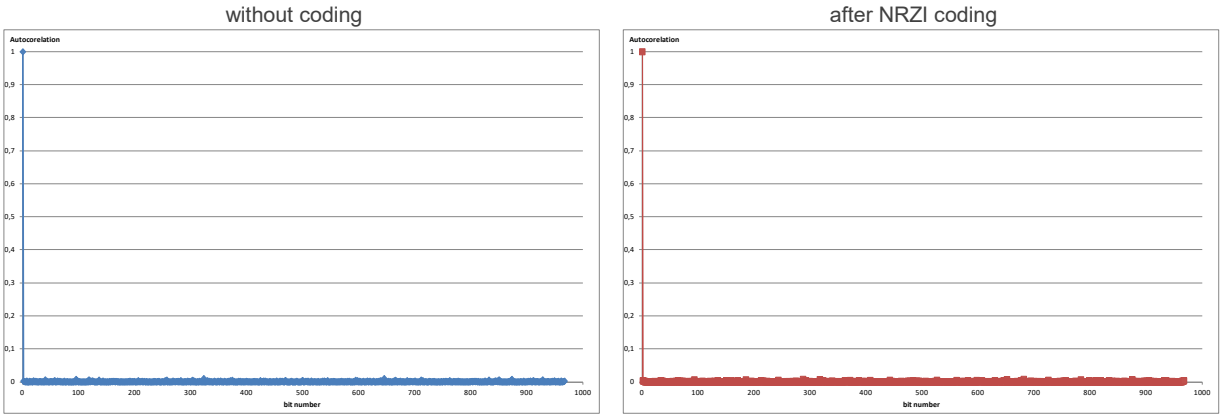

Figure 2-2: The autocorrelation function of the selected synchronisation code before and after NRZI coding

As can be seen, the NRZI coding does not affect the correlation properties of the selected synchronization code, and after coding, the second highest value has even decreased from 0,01067 for the uncoded synchronisation code to 0.00826 for the NRZI coded code.

In the next step, the NRZI coded synchronization code has been GMSK modulated. The autocorrelation function of that signal is depicted in figures 2-3 and 2-4. For better visibility, the signal was shifted in time by 2 million samples.

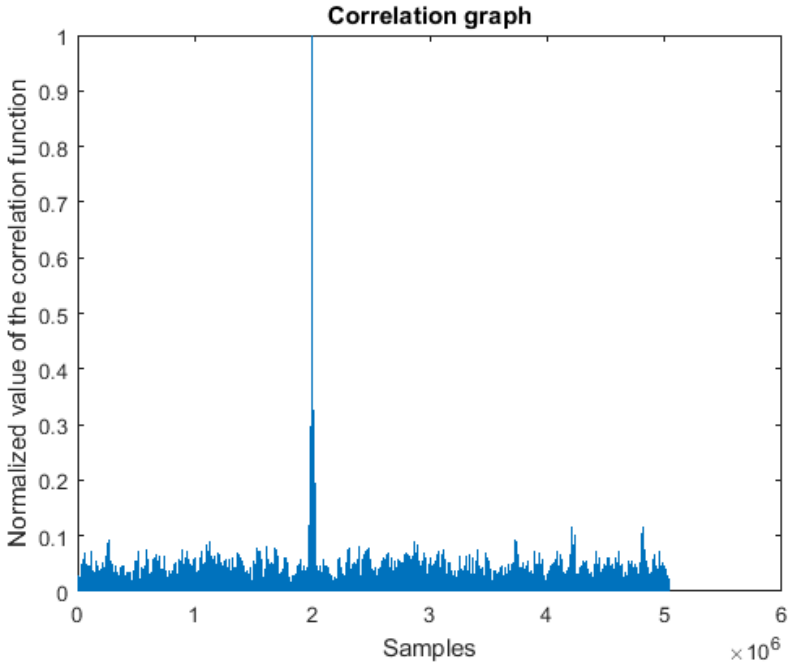

Figure 2-3: The autocorrelation function of the selected synchronisation code after GMSK modulation

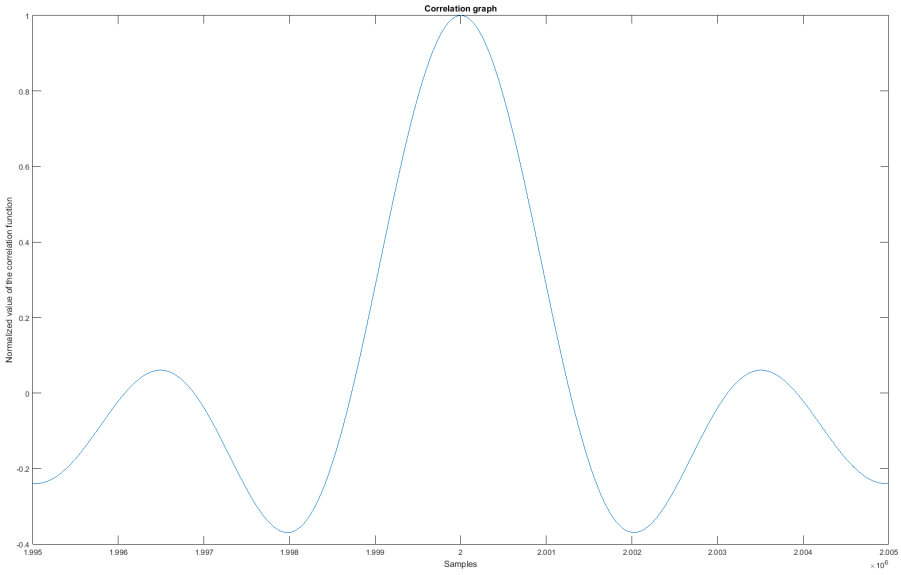

Figure 2-4: The autocorrelation function peak for the selected synchronisation code after GMSK modulation

In the next step, the GMSK modulated signal has been tested for the Doppler effect. The result was shown in figure 2-5.

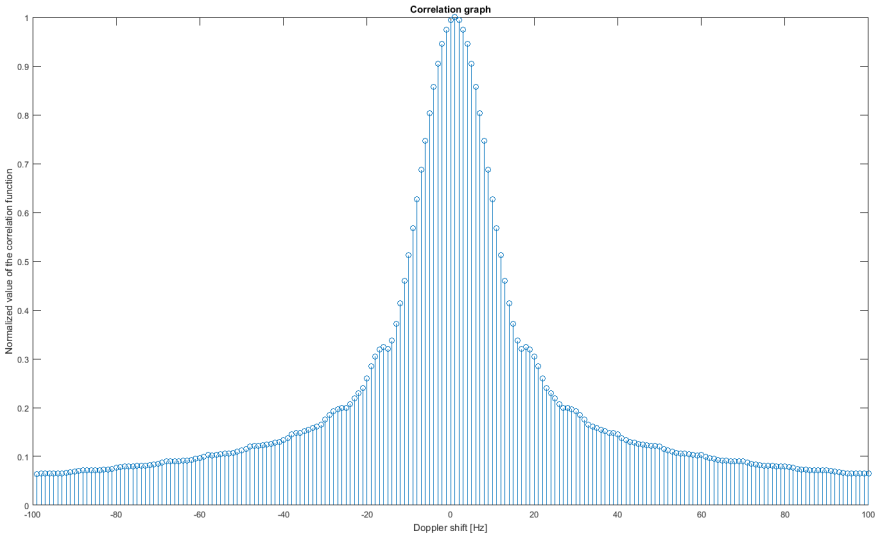

Figure 2-5: The autocorrelation function for the selected synchronisation code after GMSK modulation and with the Doppler shift

As can be seen, the selected synchronisation code of length 968 bits after NRZI coding, GMSK modulation and with the Doppler shift has still good autocorrelation properties, and can be used for the purpose of R-Mode ranging measurements.

The same procedure was carried out to search codes of length 300 and 80 bits, which meet the bit stuffing criteria. Over 200 000 usable codes of length 300 bits have been found, and among them, the one (initial state 1 174 014), whose autocorrelation function has the best properties, has been selected. This code is negative binary conversion (bipolar “1” denotes binary “1” and bipolar “-1” denotes binary “0”) of the imaginary part of the generated Gold code. For this code, the second highest value is 0.01138 for the NRZI coded code.

The selected synchronization code with initial state 1 174 014 and length 300 bits is:

0,1,0,1,1,0,0,1,1,0,0,1,0,0,1,0,1,0,1,0,0,0,1,0,1,1,0,1,1,0,0,1,0,1,1,0,1,1,1,1,0,1,0,1,0,1,1,0,1,
1,1,0,0,1,1,0,1,1,1,0,0,1,0,0,0,0,0,1,0,0,1,0,0,0,0,0,0,1,1,0,1,1,0,0,0,1,0,0,0,0,0,1,0,1,0,1,0,0,
0,0,0,0,1,0,1,0,0,1,0,0,0,1,1,0,0,1,0,0,1,0,0,1,0,1,0,1,1,1,1,1,0,1,0,1,0,1,0,1,0,1,0,1,1,0,0,1,0,1,
0,0,0,0,0,0,0,0,1,1,0,0,1,1,0,0,0,0,0,0,1,0,0,0,1,1,1,0,1,1,1,1,0,0,0,1,0,1,1,1,1,0,1,1,1,1,0,0,0,
0,1,0,0,0,0,1,0,0,1,1,0,0,0,1,0,0,1,1,1,0,0,0,1,1,1,0,1,0,1,0,1,0,1,0,0,0,1,1,0,1,1,0,0,0,1,1,0,0,
0,1,0,0,1,1,1,0,0,1,1,0,0,1,0,0,0,1,1,1,1,0,0,1,1,0,1,1,0,0,0,1,1,1,0,0,0,0,0,1,1,1,1,0,0,1,1,0,0,
0,1,1,0,1,1

For the codes of length 80 bits, over 10 000 000 codes have been found which meet the bit stuffing criteria. Once again, among them, the one (initial state 4 872 582), whose autocorrelation function has the best properties, has been selected. This code is also negative binary conversion (bipolar “1” denotes binary “1” and bipolar “-1” denotes binary “0”) of the imaginary part of the generated Gold code. For this code, the second highest value is 0.01000 for the NRZI coded code.

The selected synchronization code with initial state 4 872 582 and length 80 bits is:

1,0,0,1,0,1,0,1,0,1,1,0,0,1,1,1,0,1,1,1,0,0,1,1,1,1,0,1,1,1,1,0,1,1,0,0,0,1,0,0,0,1,1,0,0,1,1,1,1,
0,0,1,1,0,1,0,1,0,0,0,0,1,0,0,0,1,1,1,0,1,1,0,0,0,1,1,1,1,0,1

2.3 The navigation message structure

In below tables, the R-Mode navigation message structure for 1, 2 and 5 slots, designed for the purpose of the measurement tests, are shown.

Table 2-3: AIS Message 26 structure for the 1 slot message

Parameter	**Number of bits**	**Value/Description**
Message ID	6	011010
Repeat indicator	2	00
Source ID	30	000000001001111110011001110100 (AIS test station MMSI)
Destination indicator	1	0
Binary data flag	1	1
Application identifier	16	0000 0000 01 00 1010 (R-Mode 1 slot)
Station Health	8	00000000 (Not yet specified – for future use)
Gold Code	80	10010101011001110111001111011110110001000110011110 011010100001000111011000111101
Spare	4	0000
Communication state	20	00000000000000000000 (Not used during tests)
Sum	168	

Table 2-4: AIS Message 26 structure for the 2 slots message

Parameter	**Number of bits**	**Value/Description**
Message ID	6	011010
Repeat indicator	2	00
Source ID	30	000000001001111110011001110100 (AIS test station MMSI)
Destination indicator	1	0
Binary data flag	1	1
Application identifier	16	0000 0000 01 00 1011 (R-Mode 2 slots)
Station Health	8	00000000 (Not yet specified – for future use)
Gold Code	300	01011001100100101010001011011001011011110101011011 10011011100100000100100000011011000100000101010000 00101001000110010010010101111010101010101100101000 00000110011000000100011101111000101111011110000100 00100110001001110001110101010100011011000110001001 11001100100011110011011000111000001111001100011011
Spare	8	00000000
Communication state	20	00000000000000000000 (Not used during tests)
Sum	392	

Table 2-5: AIS Message 26 structure for the 5 slots message

Parameter	Number of bits	Value/Description
Message ID	6	011010
Repeat indicator	2	00
Source ID	30	000000001001111110011001110100 (AIS test station MMSI)
Destination indicator	1	0
Binary data flag	1	1
Application identifier	16	0000 0000 01 00 1110 (R-Mode 5 slots)
Station Health	8	00000000 (Not yet specified – for future use)
Gold Code	968	00000110011010110000000111101100101101110110001111 001110100000000010010011001011000110001010010101100 11101100110100111101101111001100001000000111100101 10110001000101010001010001101100100110111000100100 01001100000001101000101101001001110100000000110011 00101110110010110010011101001010100110110000011001 00110101010100101010001001001010000101010111101001 00000110010100010000000010101101100101000011000101 01010001110000110110111000010001100110010001001101 10001110100111000011100110110000000111001011100101 1 10001011110101101010111001001011110111001111000010 01001010111100011100000000000000110010101011000011 11010001011001001000000000001110001110000101011100 1 00011101100110100110010001011000010101011110101100 00111001010110100101010101011100111010000110100111 00111101100000111010011011110111001001101011010011 01011011010111011110101000101010110001100110001001 11010110111001101010101100100011001010001100111000 11101000010011100111100110000000111100000100010111 0111101011010111 11
Spare	12	000000000000
Communication state	20	00000000000000000000 (Not used during tests)
Sum	1064	

3 Distance determination accuracy in the R-Mode system

3.1 Method of determination the distance accuracy

The accuracy of distance determination in the TOA method is directly related to the duration of a single symbol, and thus to the transmission speed rate and the speed of light. In the AIS system, data transmission rate is 9600 bit/s, which gives an accuracy of approx. 150 km, which of course is unacceptable. By introducing oversampling of the signal, we can significantly increase this accuracy, as determined by the formula:

$$Acc = \frac{T_S \cdot c}{L_p \cdot 2} \tag{3-1}$$

where: Acc – accuracy,

T_S – symbol duration time,

L_P – number of samples per symbol,

c – speed of light.

Assuming that the AIS signal will be oversampled at 50 MHz (5208.3 samples per 1 AIS bit), according to (3-1) it is possible to obtain the accuracy of distance determination at the level of 3 meters. Of course, such accuracy can be obtained for the appropriate received signal levels. In order to determine the dependence of accuracy on the received signal level, we should start from determining the limit of the received signal level (receiver sensitivity):

$$S = \frac{E_b}{N_0} + 10 \cdot log(R_s) + 10 \cdot log(k) + N_0 + NF \tag{3-2}$$

where: S – signal level in dB,

E_b/N_0 – energy per bit to noise power spectral density ratio (9 dB for AIS),

R_S – modulation speed rate (9600 sym/s for AIS),

k – number of bits per symbol (1 symbol for AIS),

N_0 – noise power spectral density (-174 dBm),

NF - Noise Figure (18 dB for the AIS receivers).

The noise variance σ is given by:

$$\sigma^2 = \frac{S \cdot L_p}{k \cdot \frac{E_b}{N_o}} \tag{3-3}$$

Assuming that the synchronization code will have the L_S symbol length, after its oversampling L_P fold we will obtain an extended synchronization sequence with the length of $N = L_S \cdot L_P$ symbols. When determining the autocorrelation function for such a sequence in the presence of noise, it should be remembered that according to the normal distribution properties, the standard deviation σ_N of the sum of N normal distributions with a standard deviation σ is given by:

$$\sigma_N = \sqrt{N} \cdot \sigma \tag{3-4}$$

To obtain the highest accuracy, it is desirable that the reduction of the synchronization code autocorrelation function within 1 sample shift, which for a simplified rectangular wave can be

estimated as $2 \cdot L_S \cdot S$, was greater than the correlation between the noise and the synchronization sequence. The edge dependence can be written as:

$$2 \cdot L_s \cdot S = a \cdot \sqrt{L_p \cdot L_s} \cdot \sigma \cdot \sqrt{S} \tag{3-5}$$

where: $a = \sqrt{2} \cdot Q^{-1}(10\%)$ is the coefficient corresponding to 90% of cases for which this condition is met for a normal distribution with a standard deviation σ_N, and $Q^{-1}(x)$ is the inverse Q function ($a = 1.813$)

By transforming (3-1 to 3-5) we can obtain:

$$Acc = \frac{a \cdot c}{4} \cdot \sqrt{\frac{T_S}{L_S}} \cdot 10^{\frac{N_O + NF - S}{20}} \tag{3-6}$$

The above pattern shows that the accuracy of the determined position depends on the received signal level and the length of the synchronization code.

3.2 AIS distance determination accuracy

As it was mentioned earlier, the R-Mode project requirements indicate the AIS Message 26 for sending the synchronization codes. The 3 types of messages have been defined and they correspond to 1, 2 and 5 AIS slots respectively. The length of the synchronization code is 80 bits for 1 slot message, 300 bits for 2 slot message and 968 bits for the 5 slot message. For those lengths, on a basis of (3-6) the relation between the determined distance accuracy and the received signal level, was determined and depicted in figure 3-1.

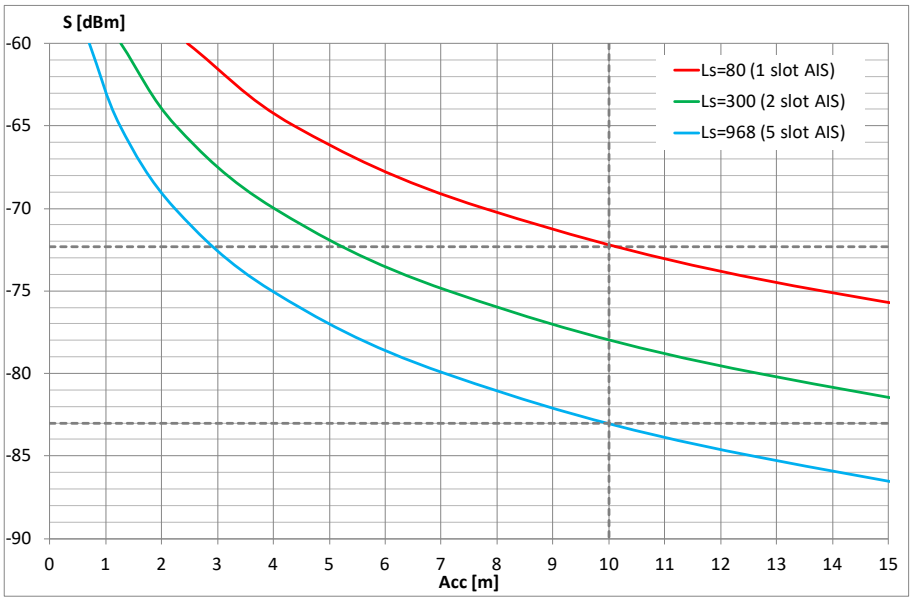

Figure 3-1: The relation between the determined distance accuracy and the received signal level

The above figure shows that achieving the R-Mode required accuracy at the level of 10 m will be possible at the received signal level in the range from approx. -72 dBm for 1 slot AIS message to approx. -83 dBm for 5 slots AIS message. For comparison, the limit of the AIS range is typically -107 dBm, so it is expected that the range of the R-Mode system will be much shorter than the AIS range.

In the next stage, the dependence of the determined distance accuracy from the AIS base station ranges was analysed. The results of radio planning carried out using the ITU-R P.1546-5 propagation model [3-1] were used, assuming the typical configuration of the AIS base station (EIRP power 46 dBm). The figures below present the results of the analysis for different heights of the base station antenna (30 m, 60 m ASL) and the ship terminal antenna (4m, 10 m, 20 m ASL).

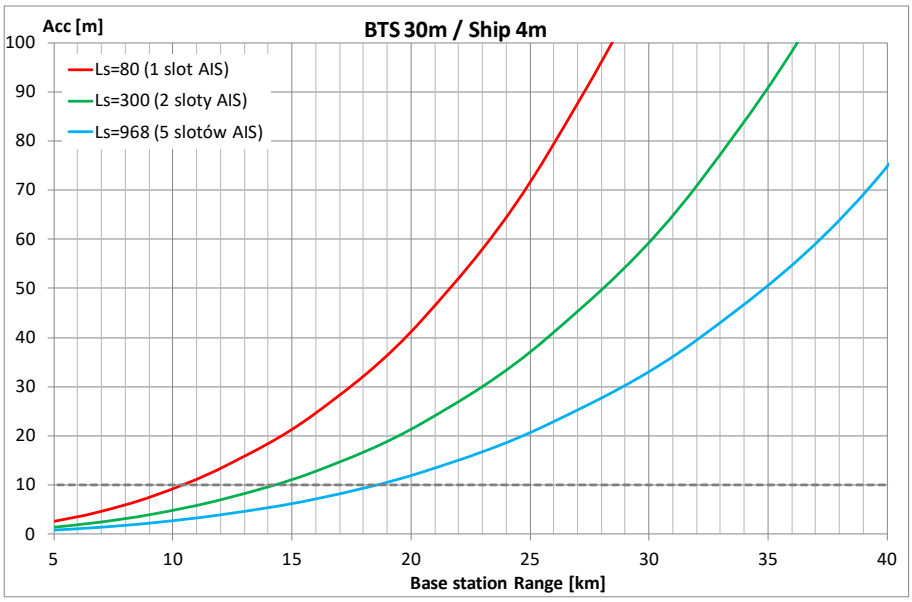

Figure 3-2: The relation between the determined distance accuracy and AIS base station range for the AIS Base station antenna height 30 m ASL and ship antenna height 4 m ASL

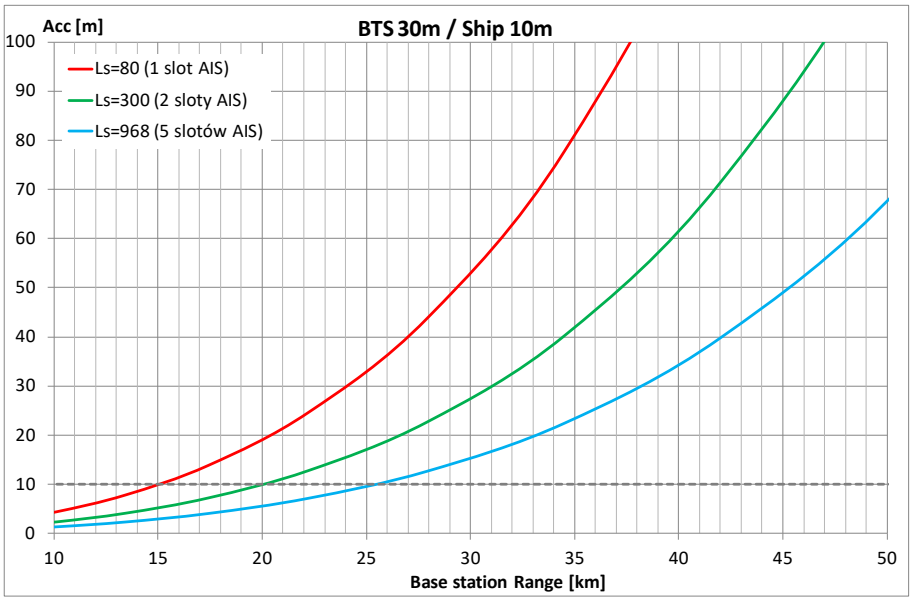

Figure 3-3: The relation between the determined distance accuracy and AIS base station range for the AIS Base station antenna height 30 m ASL and ship antenna height 10 m ASL

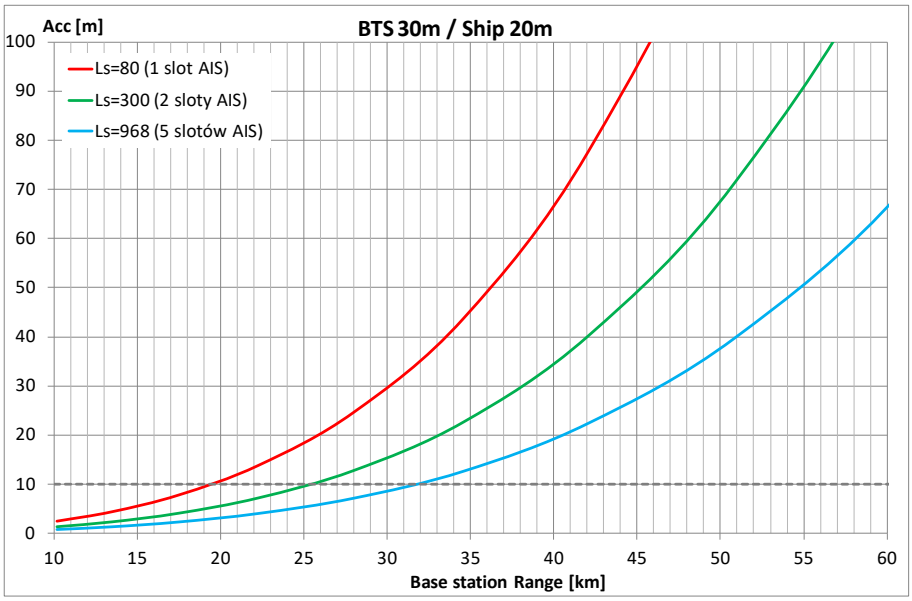

Figure 3-4: The relation between the determined distance accuracy and AIS base station range for the AIS Base station antenna height 30 m ASL and ship antenna height 20 m ASL

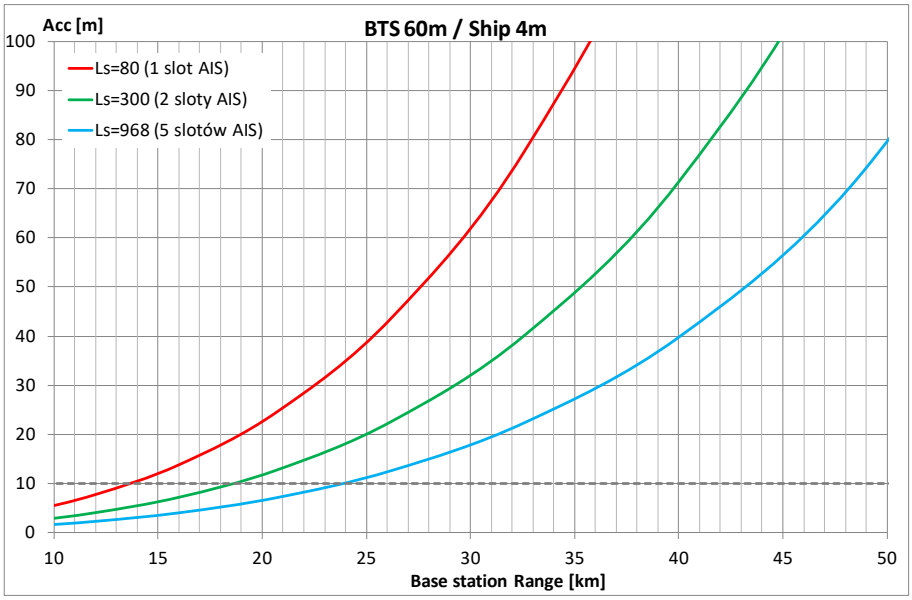

Figure 3-5: The relation between the determined distance accuracy and AIS base station range for the AIS Base station antenna height 60 m ASL and ship antenna height 4 m ASL

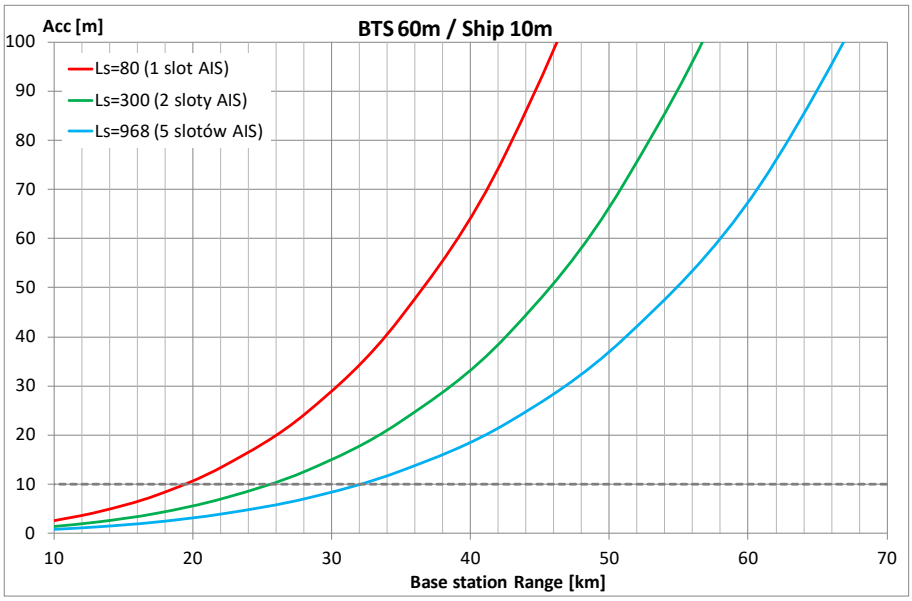

Figure 3-6: The relation between the determined distance accuracy and AIS base station range for the AIS Base station antenna height 60 m ASL and ship antenna height 10 m ASL

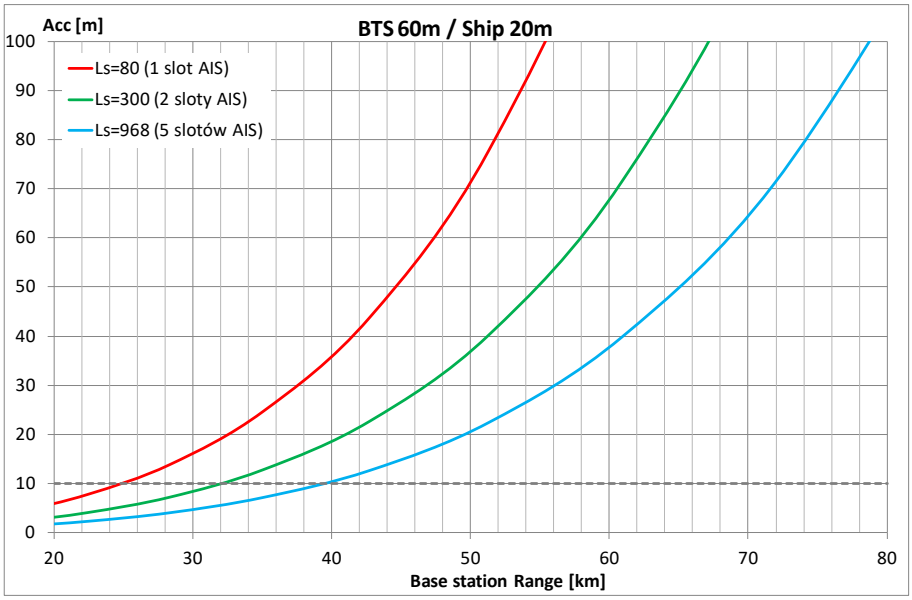

Figure 3-7: The relation between the determined distance accuracy and AIS base station range for the AIS Base station antenna height 60 m ASL and ship antenna height 20 m ASL

Having analyzed the above figures, it can be concluded that the accuracy of 10 m can be achieved in the R-Mode system with the ranges from 10 km up to 40 km. The set of those ranges has been presented in table 3-1.

Table 3-1: R-Mode ranges for 10m accuracy

Acc= 10m		AIS Ls=80	AIS Ls=300	AIS Ls=968
BTS	Ship			
30 m	4 m	10,5 km	14,5 km	18,5 km
	10 m	15 km	20 km	25 km
	20 m	19 km	25 km	31,5 km
60 m	4 m	13,5 km	18,5 km	24 km
	10 m	10 km	22,5 km	31 km
	20 m	20 km	31 km	39,5 km

4 Software implementation

In this chapter, the physical layer of the AIS system has been presented. The transmission and reception of the bit stream of data has been described. The transmission channel used for simulation has been characterized.

4.1 Transmitter

A block diagram of the transmitter is shown in Fig. 4-1.

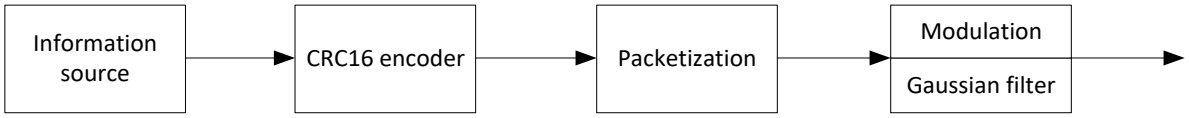

Figure 4-1: A block diagram of the transmitter part of the implemented AIS system simulator

The first step of the signal transmission process is the input data generation. An information prepared earlier is taken as the input to the CRC16 cyclic coder, where the 16 bit checksum is added. In the next step, the data are subjected to the packetization process, and after that are coded using NRZI. Data obtained from these processes are forwarded as an input to the Gaussian filter block, then they are modulated and transmitted over the radio channel. The characteristics of all of the functional blocks of the transmitter and their technical implementation have been described in the next section of this subchapter.

4.1.1 Frame format

In the transmission part of the AIS system simulator, the structure of the data frame has been defined (Fig. 4-2.). Each frame is 26.667 ms long [4-1].

Ramp Up 8 bits	Training sequence 24 bits	Start flag 8 bits	Data 168 bits	CRC16 16 bits	End flag 8 bits	Buffer 24 bits

Figure 4-2: The structure of the implemented frame for the AIS system

In the AIS system the frame consists of the following blocks [4-1]:

- A ramp up sequence which is responsible for activating the power detector,
- a training sequence, which allows the correlator in the receiver to properly determine the start of the frame,
- a start flag, which is used to detect the start of the transmission packet,
- a data block with the checksum CRC-16,
- an end flag which is used to detect the end of the transmission packet,
- a buffer, which is mainly to ensure the time reserve in order to eliminate an impact of delays due to changes of the distance between transmitting and receiving stations.

4.1.2 NRZI encoding

NRZI (Non Return to Zero Inverted) encoding is a method of transforming a binary signal to a signal that could be transmitted by a communication channel. In the two-level NRZI signal, the switching of the signal level takes place synchronously in accordance with the clock signal if the bit to be transmitted has a value 1, and if the bit to be transmitted has a value 0, the value of the physical signal is not changed. The visualization of the transmitted bit sequence and the corresponding signal is shown in Fig. 4-3.

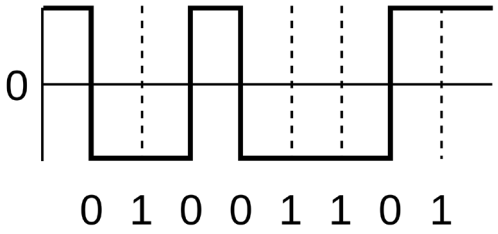

Figure 4-3: Transmitted bit sequence and the corresponding signal

4.1.3 Modulation and filtering

The GMSK modulation is the only type of modulation defined in the AIS system. In the modulator, a filter with a gaussian impulse response was used. The filter can be described with the following formula:

$$h(t) = \frac{1}{\sqrt{2\pi}\cdot\delta} \cdot exp^{\frac{-t^2}{2\delta^2}} \quad (4\text{-}1)$$

$$\delta = \frac{\sqrt{\ln(2)}}{2\pi\cdot BT} \quad (4\text{-}2)$$

The value of the filter coefficient was set to BT=0.3, where the coefficient is related to the bandwidth of the Gaussian filter B and the time period T. The signal that has been modified in this way is less demanding for the communication channel and in this case the lesser amount of energy is required to transmit a single character.

In the Fig. 4-4., the block diagram of the GMSK modulator is presented.

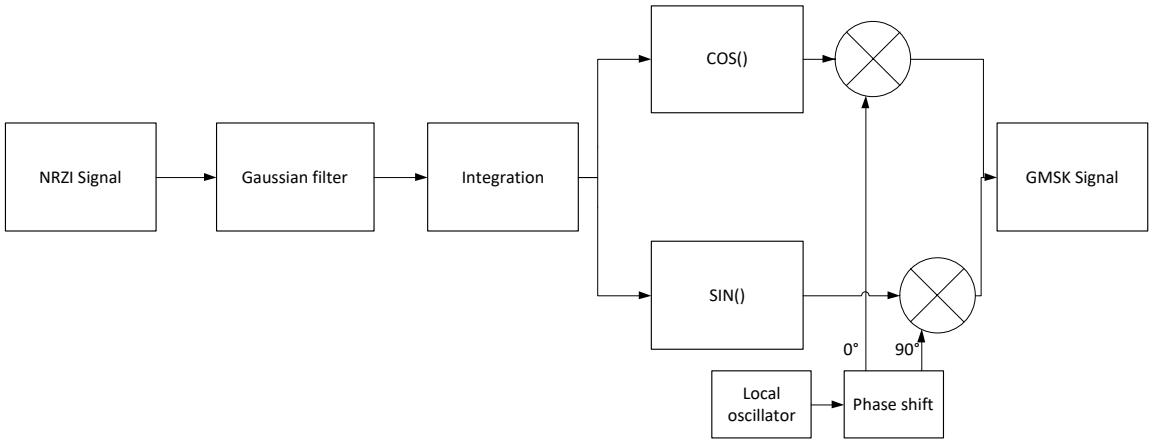

Figure 4-4: A block diagram of the GMSK modulator

4.2 AWGN channel

AWGN is a basic model of a noisy transmission channel which can be used to describe a lot of random processes. The name "AWGN" can be "deciphered" in the following way:

- A - additive, because it is possible to add noise which can be generated by the internal devices of the system,
- W - white, because it has the same power in the entire system bandwidth,
- G - Gaussian, because it has a uniform distribution in time domain with a zero mean value.

AWGN is described by the following probability distribution:

$$p(u) = \frac{1}{\sigma_u\sqrt{2\pi}} e^{-\frac{u^2}{2\sigma_u^2}} \tag{4-3}$$

To ensure the appropriate signal/noise level, it is first necessary to calculate noise variance which - for the Gaussian distribution – is σ_u^2. After some transformations, the formula for Gaussian noise variance can be presented as follows:

$$\sigma_u^2 = \frac{S \cdot L}{mod\_id \cdot \frac{E_B}{N_0}} \tag{4-4}$$

where:

- S - signal power,
- L - number of samples per symbol,
- mod_id - number of bits per single symbol,
- E_B - energy of bit,
- N_0 - noise spectral density.

If the noise variance is known, it is possible to obtain the required signal to noise ratio during the simulations.

4.3 Receiver

The block diagram of the AIS receiver is depicted in fig. 4-5.

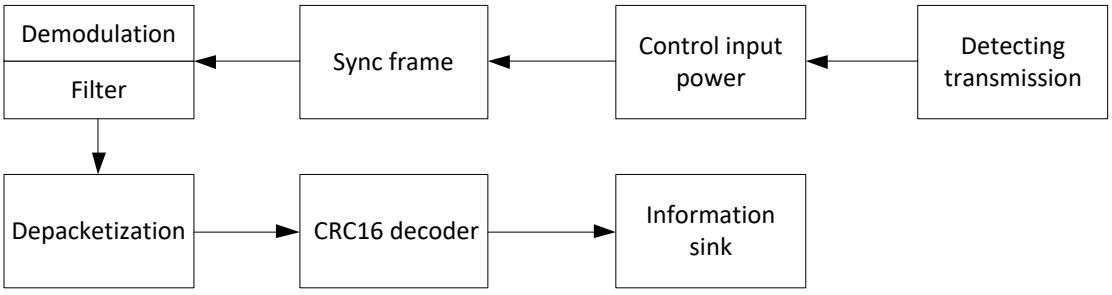

Figure 4-5: AIS receiver block diagram

The first step of the reception procedure is the transmission detection. It is performed using a power detector. The subsequent stages are: time synchronization, phase synchronization and amplitude synchronization. After that, the signal is subjected to a filtration process. Then, the bits are fed to the depacketizer block which selects only the bits that belong to the data block. In the final phase, the data is demodulated. Their correctness is verified using the cyclic code CRC-16 and the received information is determined.

4.3.1 Power detector

In the first stage of the receiving process it is necessary to confirm that radio transmission actually takes place. The transmission detection comes down to checking whether the average signal power in the transmission channel is above the designated threshold, or not. The block diagram of the power detector can be depicted as in Fig. 4-6.

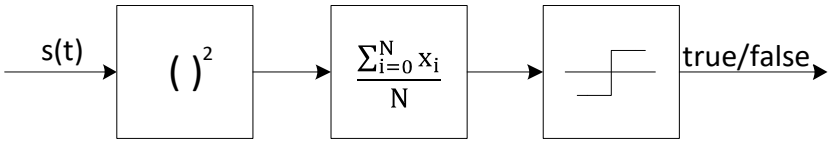

Figure 4-6: Power detector block diagram

First, the system writes N samples from the radio channel into the receiver's memory. Packets s(t) prepared in this way are then fed into the power detector's input where they are squared and averaged. The result of this operation is an input of a decision-making system which verifies if the channel signal power is greater than the assumed threshold. If this is the case, the receiver initiates time synchronization process, if not – transmission detection has to start over.

4.3.2 Time synchronization

When the receiver detects a transmission, it becomes necessary to determine the position of the transmitted frame. The block diagram of the module that performs such a procedure is presented in Fig. 4-7

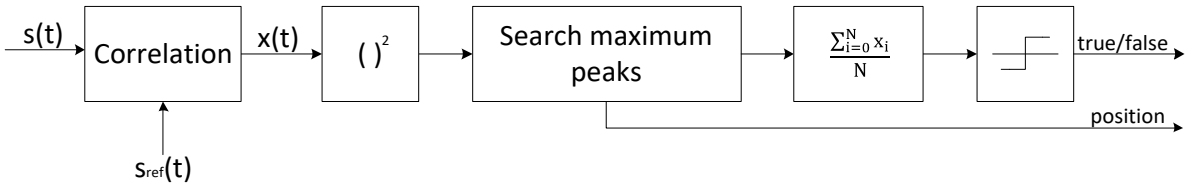

Figure 4-7: Time synchronization block diagram

As soon as there are enough samples in the receiver's memory, the time synchronization algorithm starts. First, the received signal is correlated with a known reference signal.The resulting values are squared. In the next stage, the algorithm searches for N neighbouring peaks whose average value is maximum (the value of N depends on the number of samples per single symbol). The position of the located peaks is stored in the memory and this calculated value is processed by a decision-making block which compares it with the

designated threshold. If the value is greater than that threshold, the receiver assumes the frame is being transmitted and starts obtaining the data from the transmission channel. Otherwise, the receiver resumes the transmission detection procedure.

4.3.3 Phase synchronization

After the frame's position has been determined and the sufficient amount of data has been gathered, in the next step, the phase of the signal needs to be calculated. To do so, a device that works according to the following block diagram (fig. 4-8) has been implemented.

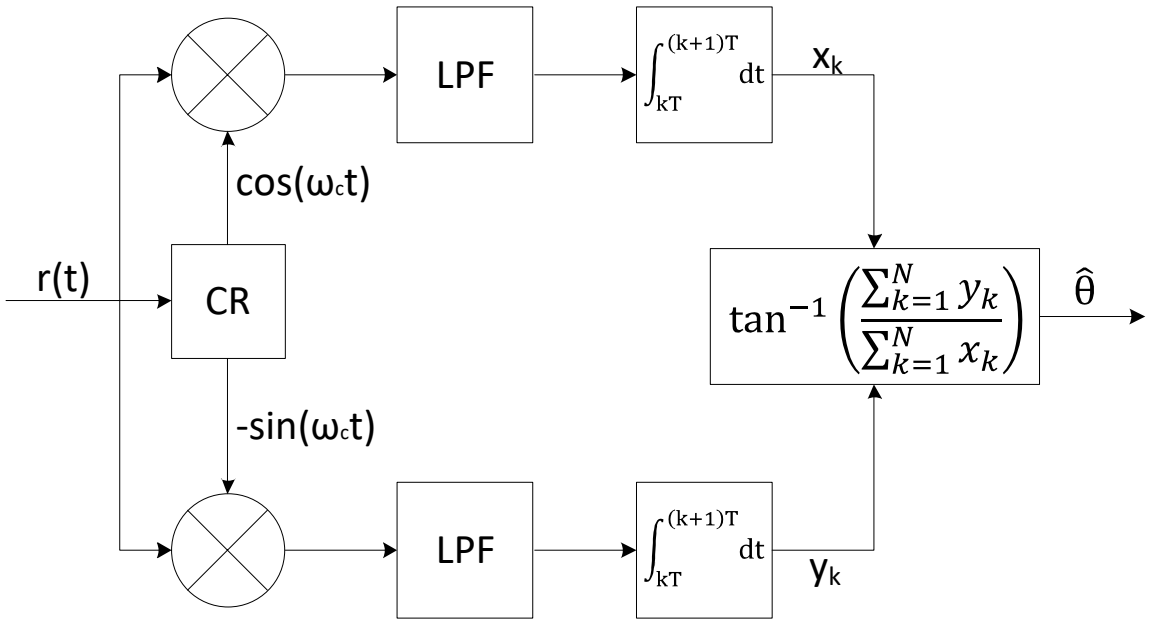

Figure 4-8: Phase synchronization module - block diagram

The received signal r(t) at the phase synchronization module's input is multiplied by the signal $cos\omega_c t$ (upper branch) and the signal-$sin\omega_c t$ (lower branch). The frequencies of these signals are equal to the carrier frequency. The resulting impulses are then fed into the low-pass filter's input. As a result, two tables are created into which the position of the received symbols on the Re axis (x_k) and Im axis (y_k) is written. In the next step, each of the tables is averaged, which allows to calculate the position of the resulting symbol and to determine its phase (which is equal to: arctg (symbol's position on the Im axis/symbol's position on the Re axis)).

4.3.4 Amplitude synchronization

The module responsible for the amplitude's determination works according to the similar algorithm as the one described in the previous subchapter. The only difference is the last component in which the actual parameter is calculated. In case of the amplitude synchronization, the calculation to be made is a squared root of the sum of squared values from tables x_k and y_k. The amplitude synchronization module is depicted in Fig.4-9.

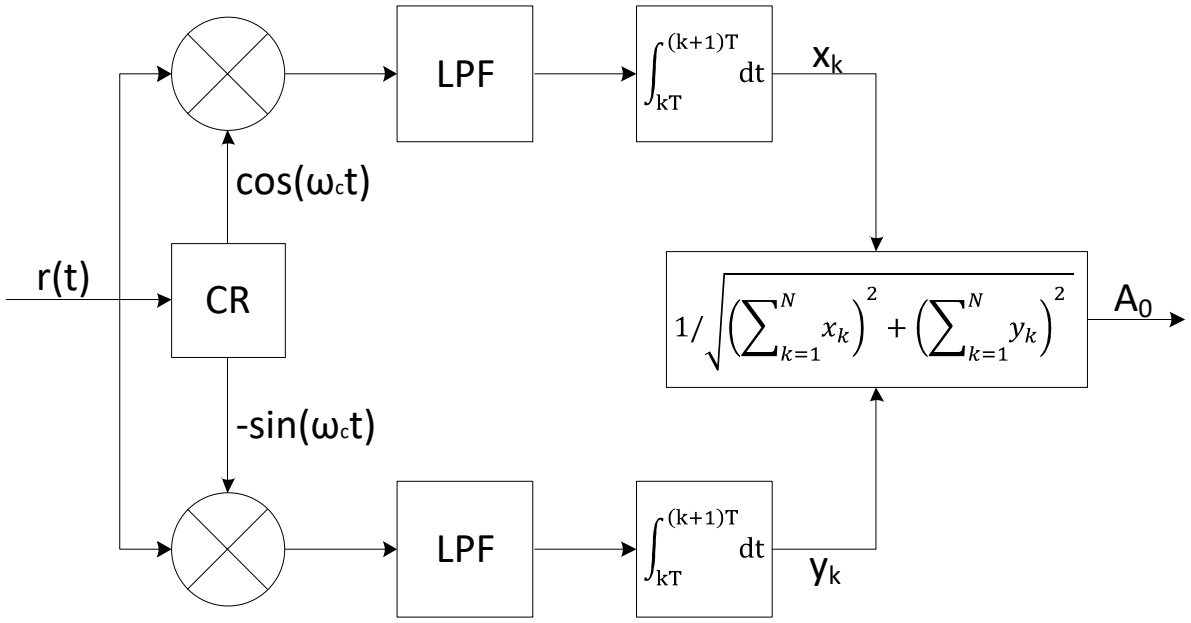

Figure 4-9: Amplitude synchronization module - block diagram

4.3.5 Demodulation

The last stage of the signal processing in the receiver is its filtering and demodulation. In the AIS simulator, the GMSK demodulator is implemented, which is shown in Fig. 4-10.

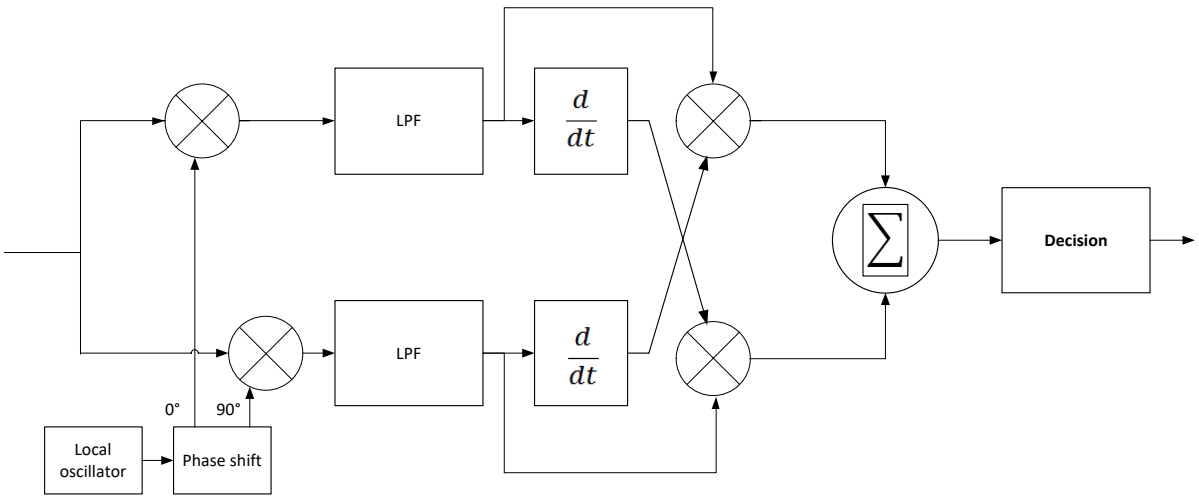

Figure 4-10: Block diagram of the GMSK demodulator

The received signal is multiplied by the signal $cos\omega_c t$ (upper branch) and the signal-$sin\omega_c t$ (lower branch). The frequency of these signals is equal to the carrier frequency. The impulses are then fed into the LPF filter's input. Then the samples go to the integrator module. The last element of the demodulator is the decision system, where the signal is decoded.

4.4 Simulation tests

The charts presented in the subchapters below are based on the results acquired from the AIS system simulator. The aim of these results is to show the correctness of the implemented simulator operation, and to show the results of the conducted research in the aspect of accurate correlation and some others.

4.4.1 Obtained BER, BLER and synchronization error curves

In Fig. 4-11. a Bit Error Rate (BER) curve generated in the AIS system simulator has been presented. It is in compliance with the theoretical BER curve for GMSK modulation. Additionally, in Fig. 4-12. a Block Error Rate (BLER) curve has been presented, with the aim to show the ratio of the incorrectly received entire data packets to all received packets.

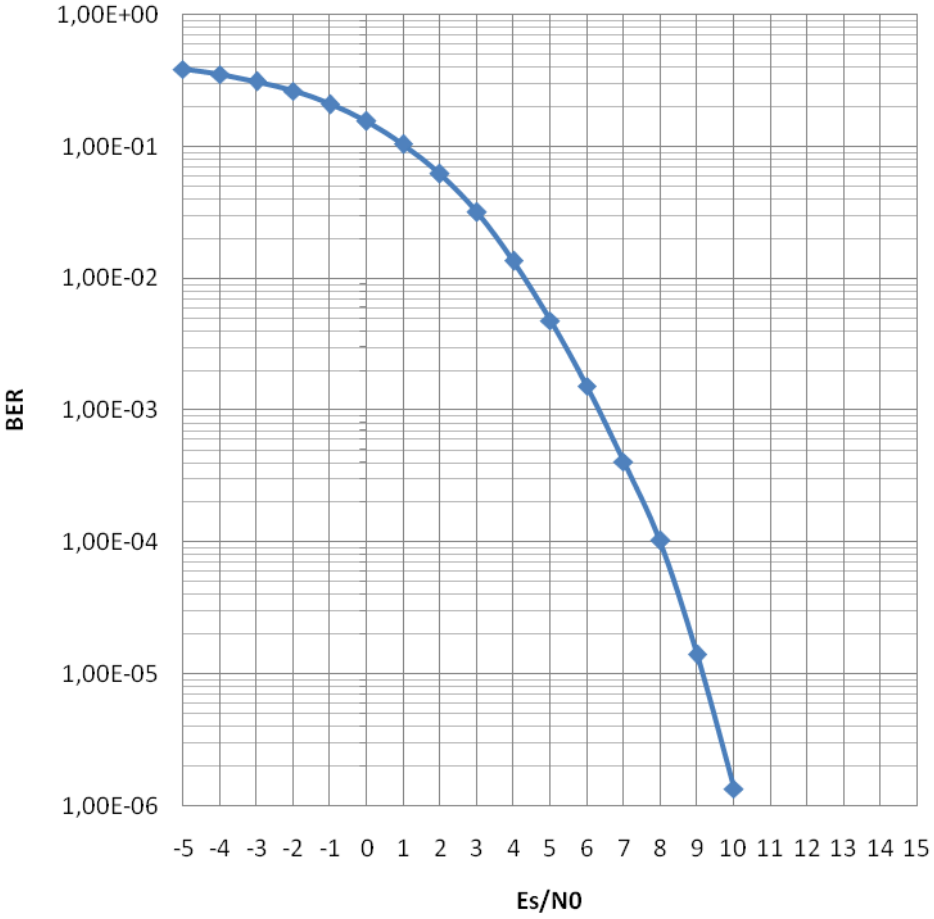

Figure 4-11: A Bit Error Rate curve for GMSK modulation in the implemented AIS system simulator

In Fig. 4-13. a synchronization error curve has been presented. It shows a ratio of the number of incorrectly determined frame positions in the receiver to the number of all frames which were subjected to the synchronization process, depending on the ratio of the energy of a single symbol to noise spectral power density. Starting from values above Es/N0 = 0 dB it was possible to achieve very accurate synchronization when receiving data.

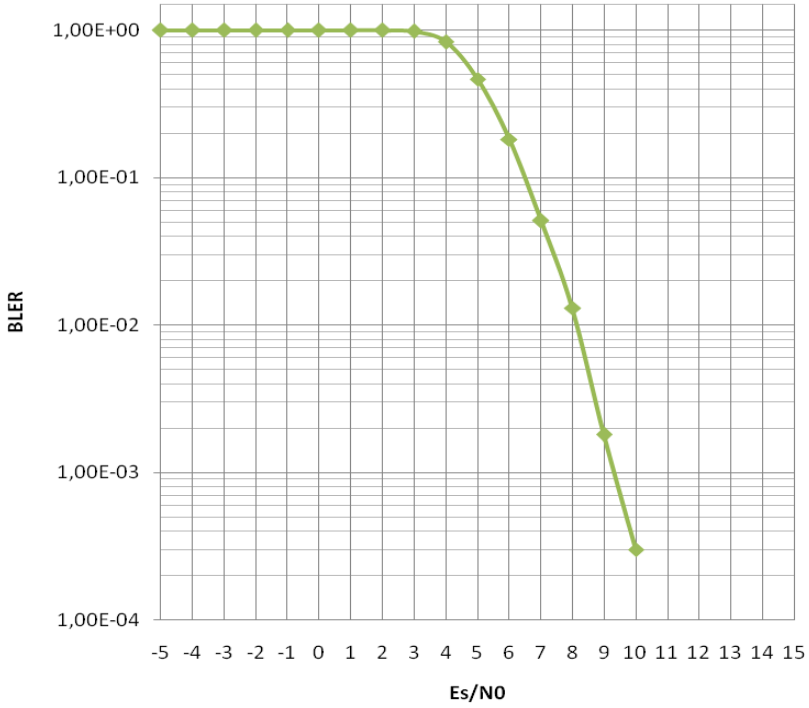

Figure 4-12: A Block Error Rate curve for GMSK modulation in the implemented AIS system simulator

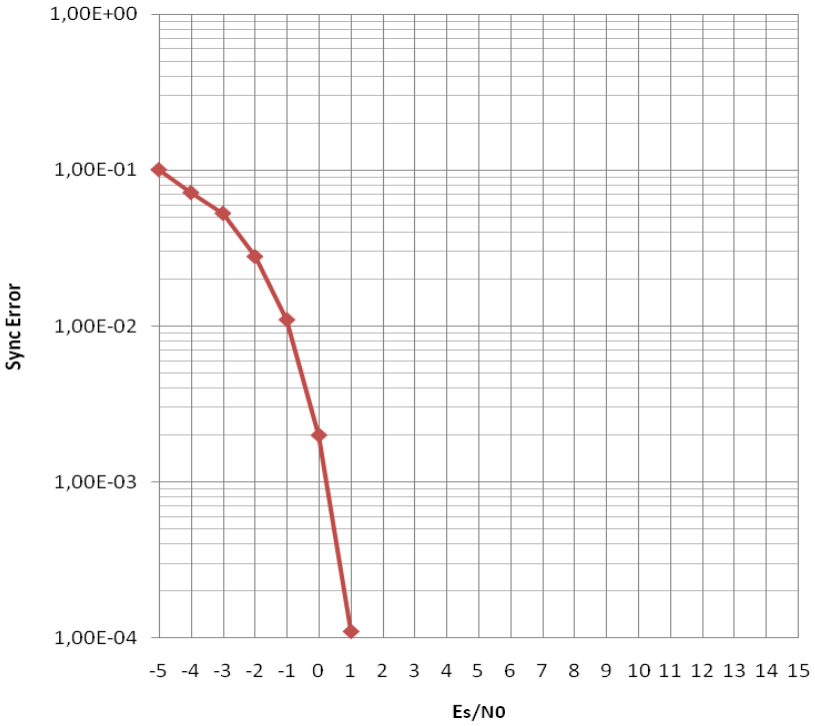

Figure 4-13: A synchronization error curve for GMSK modulation in the implemented AIS system simulator

4.4.2 Correlator based on an oversampled signal

There are two correlators implemented in the AIS system receiver. The first one uses a correlation of the received signal with the previously known reference signal. With that, determination of the transmitted frame position is possible. The second correlator uses an oversampled signal. The correlation is calculated, and after that the correlator searches for the main peak. This allows to determine the distance between the transmitter and the receiver with the accuracy of one sample, i.e. ±3 meters. In Fig. 4-14. a relation between the ratio of the single symbol energy to noise spectral power density and an accuracy of correlation calculated per one sample has been presented.

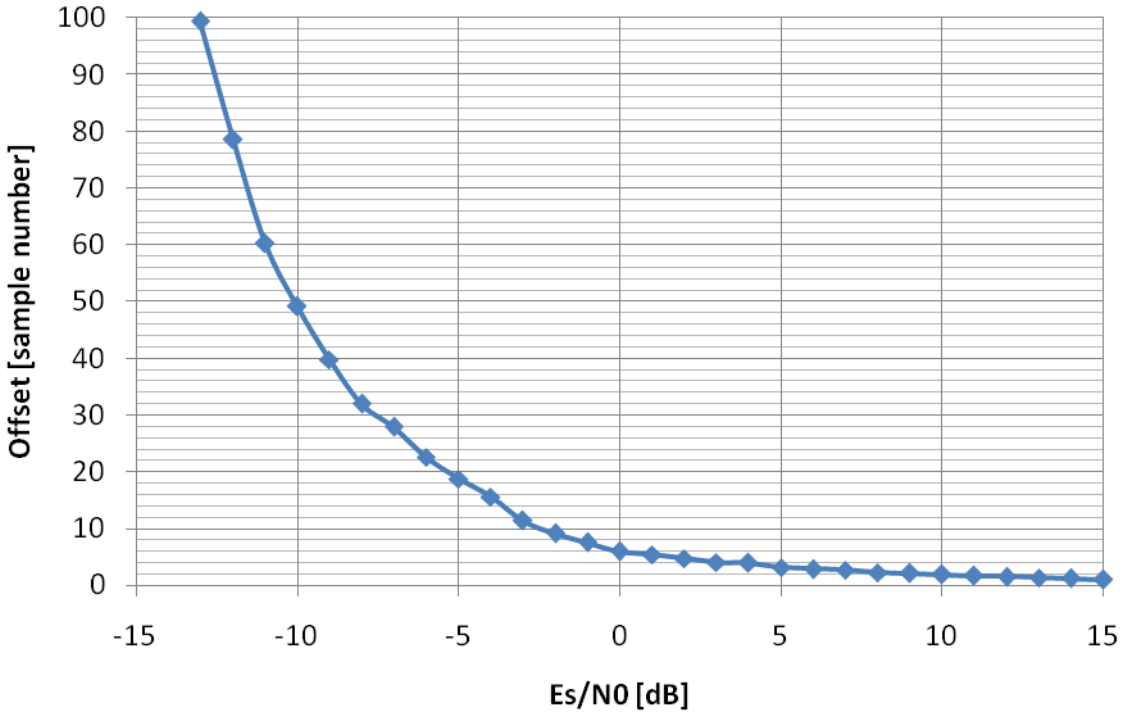

Figure 4-14: A chart showing a dependency between the ratio of the energy of a single symbol to noise spectral power density and an accuracy of correlation calculated per one sample

The accuracy of a one sample for determining the distance between the transmitter and the receiver was achieved during the simulation tests starting from the value of Es/N0 ratio equal to 10 dB.

In Figures 4-15 – 4-18 below, the results of correlation depending on the Es/N0 ratio value has been presented.

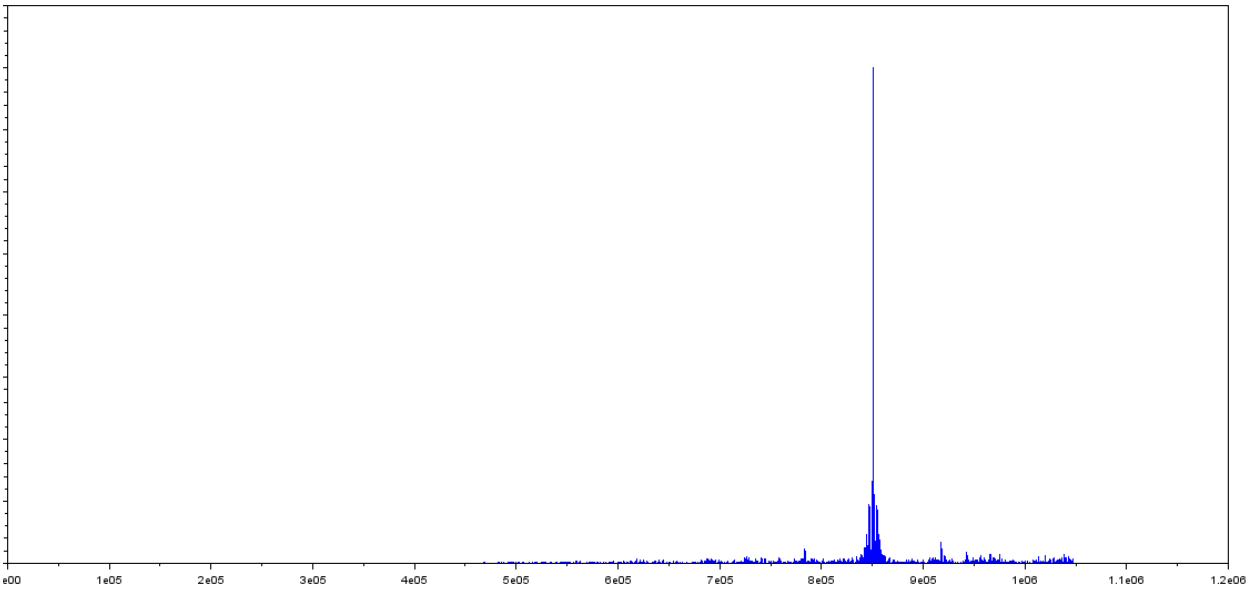

Figure 4-15: Correlation function for Es/N0 = 10 dB

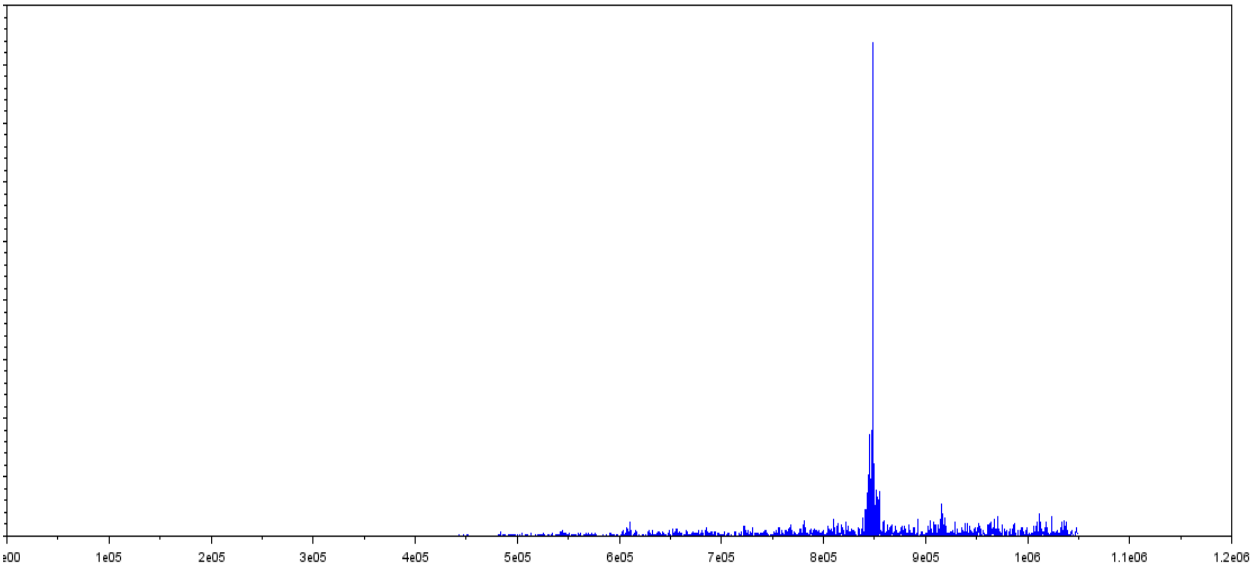

Figure 4-16: Correlation function for Es/N0 = 8 dB

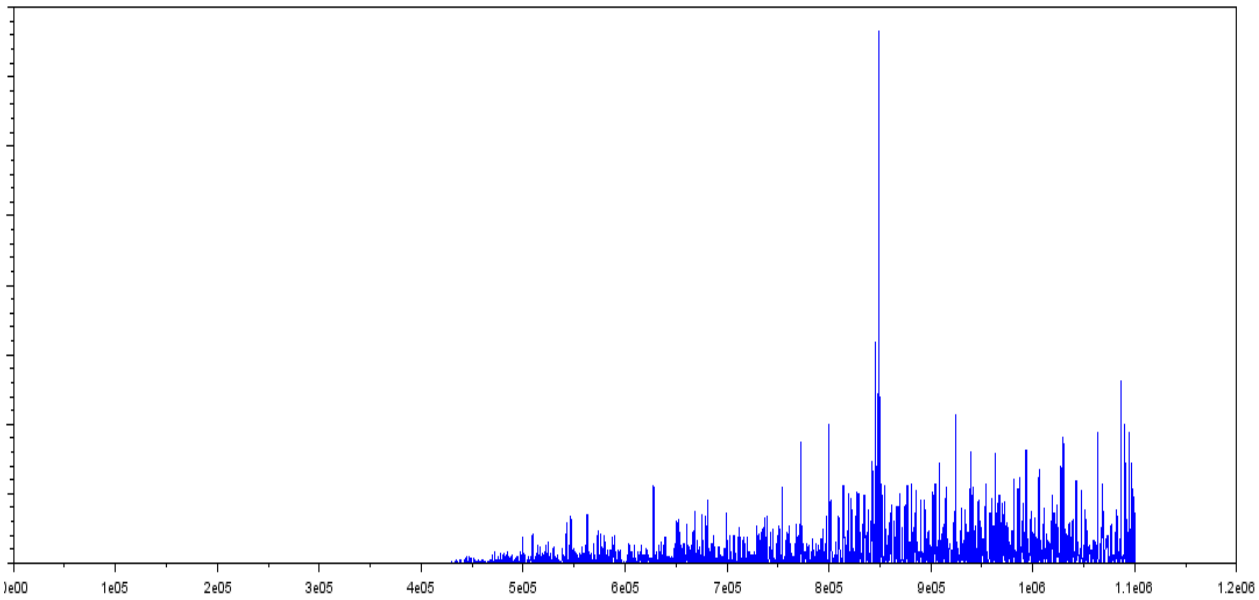

Figure 4-17: Correlation function for Es/N0 = -3 dB

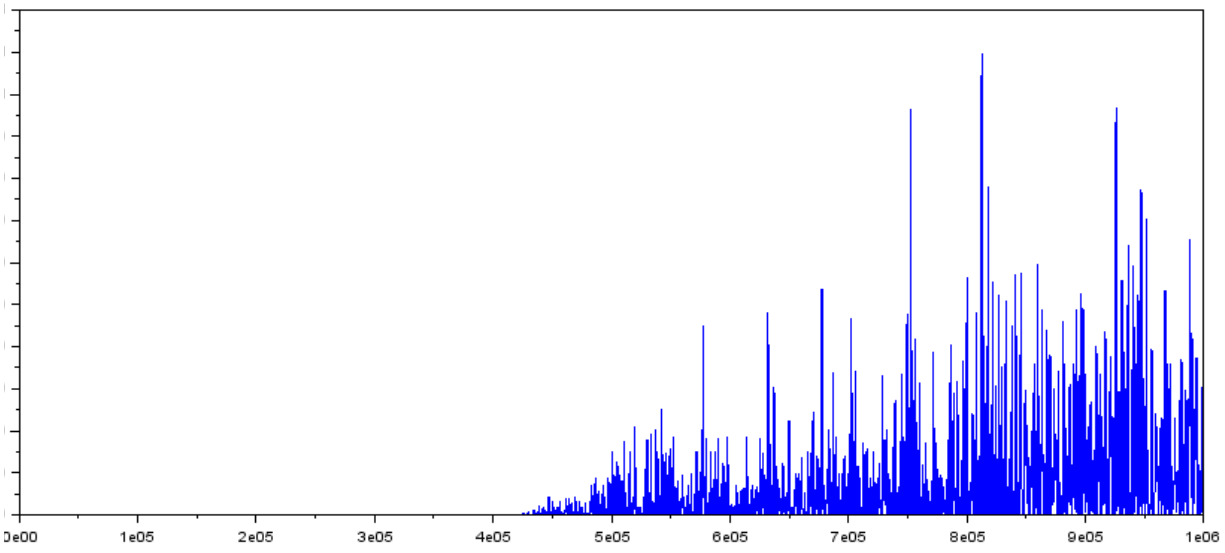

Figure 4-18: Correlation function for Es/N0 = -12 dB

4.5 Hardware implementation

There are two main hardware elements that have been selected for the purpose of implementation works based on our experience. The first one is the USRP (Universal Software Radio Peripheral) hardware platform provided by National Instruments. The second component is a Rubidium Time and Frequency Reference. They have been characterized in the following subsections.

4.5.1 USRP platform

The NI's USRP devices are software defined radios (SDR) used for prototyping wireless communication systems. USRP is a tunable RF transceiver with high-speed analog-to-digital and digital-to-analog converters for streaming baseband I and Q signals to a host PC over 1 Gigabit Ethernet. The main advantages of the USRP are flexibility, functionality and affordability that make this platform suitable for fast prototyping and testing of new wireless solutions.

USRP hardware implements a direct conversion analog front end with high-speed analog-to-digital converters (ADCs) and digital-to-analog converters (DACs) featuring a fixed-personality FPGA for the digital downconversion (DDC) and digital upconversion (DUC) steps. The receiver chain begins with a highly sensitive analog front end that can receive very small signals and digitize them using direct downconversion to in-phase (I) and quadrature (Q) baseband signals. Downconversion is followed by high-speed analog-to-digital conversion and a DDC that reduces the sampling rate and packetizes I and Q for transmission to a host computer using Gigabit Ethernet for further processing. The transmitter chain starts with the host computer where I and Q are generated and transferred over the Ethernet cable to the USRP hardware. A DUC prepares the signals for the DAC after which I-Q mixing occurs to directly upconvert the signals to produce an RF frequency signal, which is then amplified and transmitted.

It was decided to use the USRP 2920 model in the designed test-bed. In picture 4-19, NI USRP 2920 device is depicted.

Figure 4-19: NI USRP 2920 module

The most important parameters of the USRP 2920 are specified below.

USRP 2920 transmitter parameters [4-2]:

- Frequency range: 50 MHz to 2.2 GHz,
- Frequency step: <1 kHz,
- Maximum output power:
  - 50 MHz to 1.2 GHz 50 mW to 100 mW (17 dBm to 20 dBm),
  - 1.2 GHz to 2.2 GHz 30 mW to 70 mW (15 dBm to 18 dBm),
- Gain range: 0 dB to 31 dB,
- Gain step: 1.0 dB,
- Frequency accuracy: 2.5 ppm,
- Maximum instantaneous real-time bandwidth:
  - 16-bit sample width: 20 MHz,
  - 8-bit sample width: 40 MHz,
- Maximum I/Q sample rate:
  - 16-bit sample width 25 MS/s,
  - 8-bit sample width 50 MS/s,
- Digital-to-analog converter (DAC): 2 channels, 400 MS/s, 16 bit.

USRP 2920 receiver parameters [4-2]:

- Frequency range: 50 MHz to 2.2 GHz,
- Frequency step: <1 kHz,
- Gain range: 0 dB to 31.5 dB,
- Gain step: 0.5 dB,
- Maximum input power: 0 dBm,
- Noise figure: 5 dB to 7 dB,
- Frequency accuracy: 2.5 ppm,
- Maximum instantaneous real-time bandwidth:
  - 16-bit sample width 20 MHz,
  - 8-bit sample width 40 MHz,
- Maximum I/Q sample rate:
  - 16-bit sample width 25 MS/s,
  - 8-bit sample width 50 MS/s,
- Analog-to-digital converter (ADC): 2 channels, 100 MS/s, 14 bit.

USRP 2920 has a low quality oscillator, but it can be used an external source of frequency and time using PPS and frequency reference inputs. For the purpose of building the R-Mode System test-bed, the rubidium oscillators described in the next subsection were chosen.

4.5.2 Rubidium Time and Frequency Reference

The Quartzlock E80-GPS is a GPS Disciplined Rubidium Frequency & Time Reference. The device provides a stable and accurate calibration free GPS time & frequency with multiple outputs signal formats, which is a cost effective solution for applications that require frequency reference. This reference maintains high time and frequency accuracy required for demanding applications. The additional advantage of the internal rubidium module is that there is no measurable difference between the stability when locked to GPS or in Holdover mode with measurement times up to 1000s.

The most important parameters of Quartzlock E80-GPS [4-3]:

- Frequency Stability (Allan Deviation)
  - Frequency 10MHz:
    - τ=1s ≤ 8x10^{-13},
    - τ=10s ≤ 2x10^{-12},
    - τ=100s ≤ 4x10^{-12},
- Phase Noise (SSB)
  - 1 Hz: -115 dBc,
  - 10 Hz: -140 dBc,
  - 100 Hz: -154 dBc,
  - 1 kHz: -155 dBc,
  - 10 kHz: -160 dBc,
- Harmonics: <-30dBc,
- Spurious (@100 KHz BW): <-100dBc,
- PPS Accuracy: <12ns (Pulse Width 10 millisecond),
- Timing accuracy at Holdover: Per 24 hours 1µ sec.,
- Frequency aging at Holdover mode:
  - Per day: 5x10^{-12},
  - Per month: 5x10^{-11},
- RS232 NMEA Output,
- Outputs: 10MHz (SMA), 1PPS (SMA),
- Internal battery included,
- High Gain GPS Antenna:
  - Gain: 35dB ±3dB,
  - L1 GPS, 1575.42MHz ±1.023MHz,
  - Waterproof, weatherproof.

In picture 4-20, the Quartzlock E80-GPS rubidium oscillator and high gain GPS antenna are shown.

Figure 4-20: Quartzlock E80-GPS and High Gain GPS Antenna

In addition to providing an accurate source of time and frequency for the USRP devices, the rubidium oscillator is also used to synchronization between the transmitting and receiving part of the measurement system.

4.5.3 USRP application

LabVIEW development environment provided by National Instruments was selected to control the USRP devices. LabVIEW is a graphical dataflow programming environment well suited for designing and implementing communications algorithms. At the most fundamental level, LabVIEW uses the NI-USRP driver to both specify USRP hardware configuration and send and receive properly formatted baseband I/Q data. Blocks for channel coding, pulse shaping, simulating channel impairments, creating visualizations, and more make the USRP driver API essential to most applications. Included examples offer a starting point for implementing a communications link using a variety of modulation schemes and are ready for use out of the box. LabVIEW provides the signal processing engine for the modulation and demodulation of signals streaming to and from USRP hardware.

In the R-Mode system the distance between base station and mobile station on the ship is determined using the TOA method which is based on the measurement of radio signal propagation time. Therefore, the key issue is to ensure transmission and reception start of R-Mode messages in precisely defined moments of time. For this purpose, the triggers are utilized in the USRP modules. They are used for generation and acquisition synchronization to the timestamp specified by the ‘Start Trigger Time’ properties. The ‘Start Trigger’ occurs when the onboard device timer reaches the timestamp specified by the user. Therefore, the operation of setting the trigger and data transmission/reception must be performed periodically - in a loop.

In pictures 4-21 and 4-22, the flowcharts of the transmitting and receiving applications are illustrated.

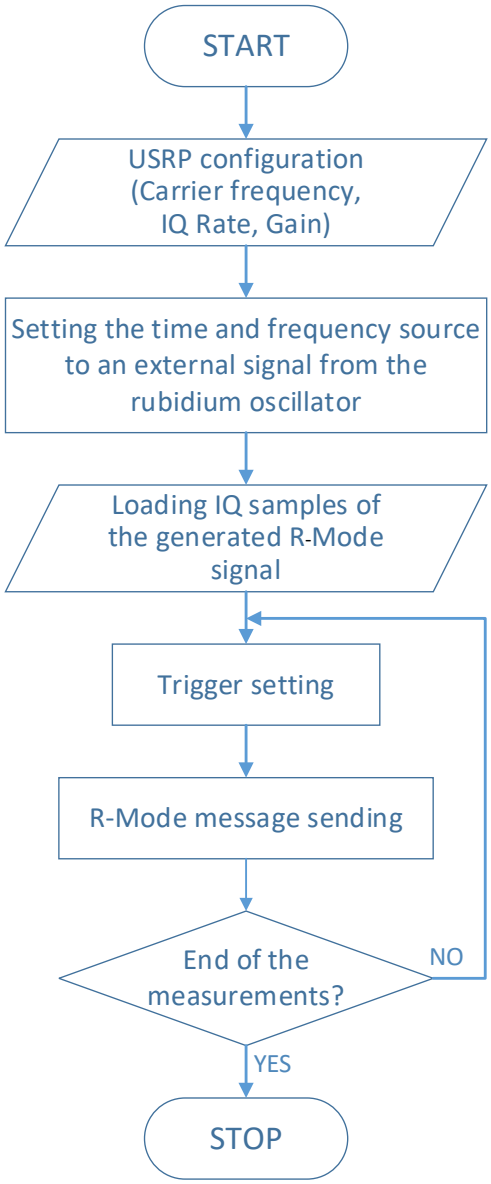

Figure 4-21: Transmitting application flowchart

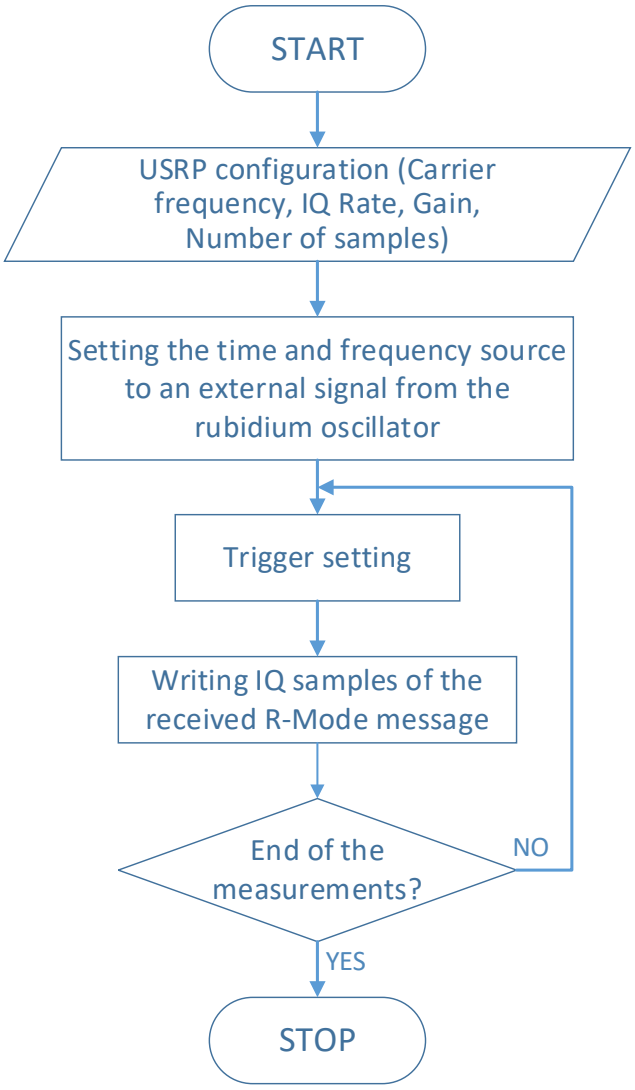

Figure 4-22: Receiving application flowchart

The designed applications allow to configure the following parameters of the USRP device:

- carrier frequency,
- IQ Rate (sampling rate),
- gain,
- number of samples,
- Start Trigger Time parameter,
- antenna port number,
- frequency of sending/receiving messages.

Applications have the following features:

- full configurability of radio parameters,
- reading/writing signals from/to the file in the form of IQ samples,
- possibility of graphical signal presentation,
- automation of measurements,
- monitoring of application work and logging of configuration and possible errors.

In order to check the correctness of the developed solution, a laboratory measurement site was prepared. In picture 4.23 the diagram of this laboratory test-bed is presented.

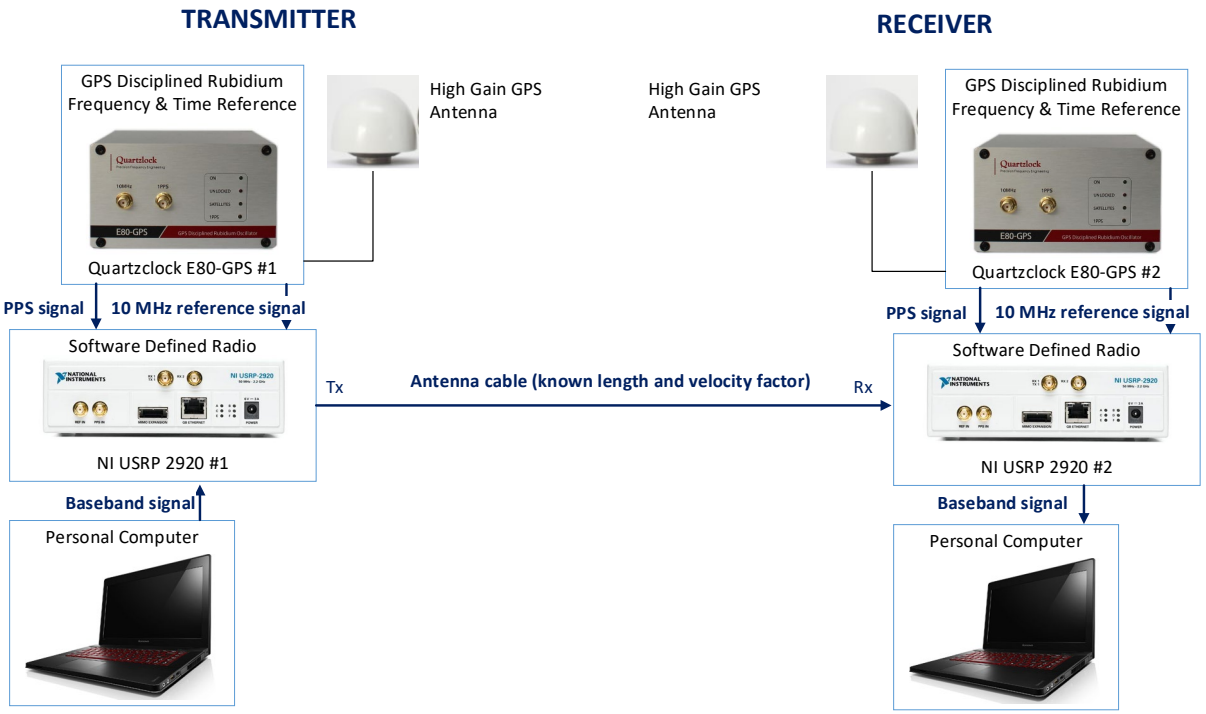

Figure 4-23: Diagram of laboratory test-bed for signal transmission time measurements

USRP modules were connected using antenna cable with known length and velocity factor. These parameters are necessary for determining the path length of electromagnetic wave. Another important issue is using the same cables (length and velocity factor) for time and frequency reference signals from the external rubidium oscillators in the transmitter and receiver. In the presented example, carrier frequency was set to 160 MHz and IQ sample rate was set to 50 MHz, and the transmitted signal was sinus at frequency of 10 kHz. The time of transmission start is equal to the time of receiving start and the offset is measured. This offset consists of USRP processing time and signal propagation delay. USRP processing time must be taken into account and it was determined using a very short cable between the USRPs (about 1 meter length). Processing time varies for different configurations of USRPs, but it is constant. After that, a measurement using a long cable (about 21 meters considering the velocity factor) was made and the obtained results were compared.

Figs. 4-24 and 4-25 present the results obtained for the connection of the transmitting and receiving USRP devices using a short cable and a long one, respectively.

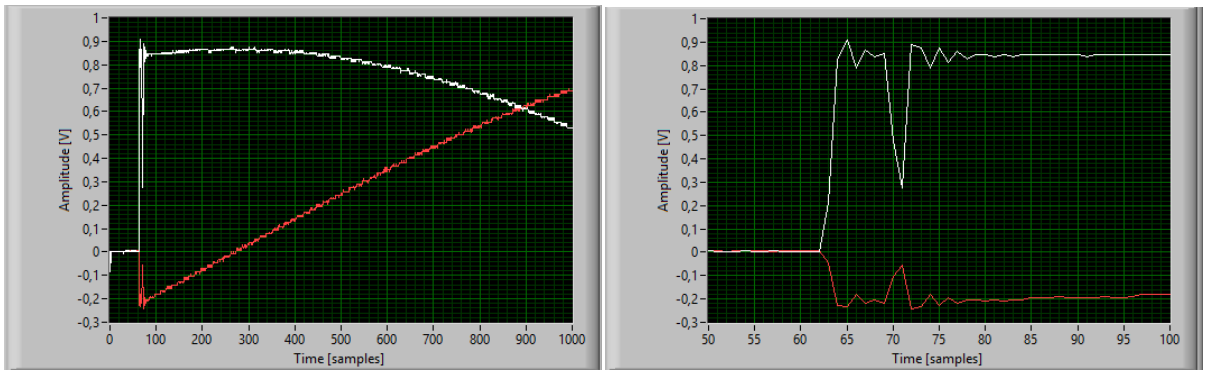

Figure 4-24: Example of signal reception delay using a short transmission cable

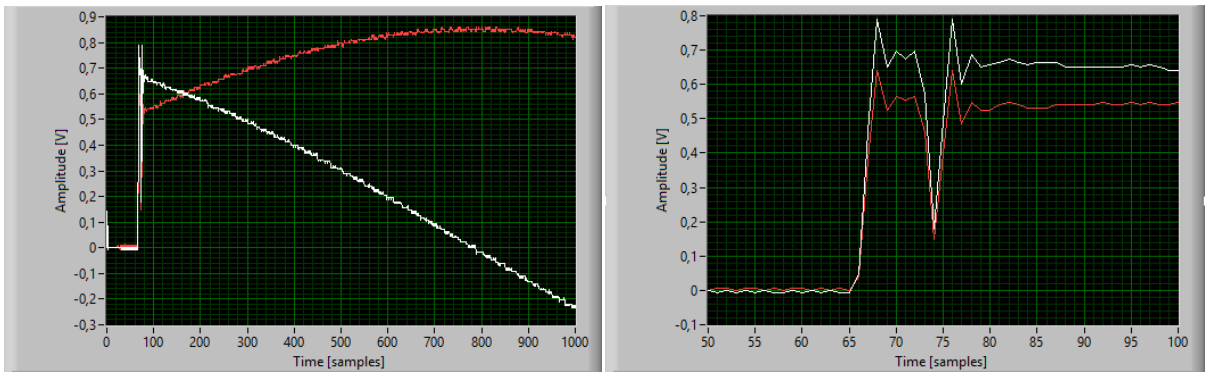

Figure 4-25: Example of signal reception delay using a long transmission cable

In the first case, the received signal starts with a sample number 62 and in the second case (long cable) it starts with a sample number 65. Difference between start sample numbers is equal to 3. In this example, the IQ sample rate was set to 50 MHz, so 1 sample corresponds to 20 ns, which corresponds to 6 meters. The obtained delay represents the distance of 18 ± 3 meters and therefore it matches with predictions.

It should be noted that if we use a new USRP model (with IQ sampling rate 200 MHz) then 1 sample will correspond to 1.5 m, so we can improve the resolution and distance accuracy.

Another examined issue was the impact of propagation attenuation on the recorded signal. The amplitude of the signal received by the USRP has the values from -1 to +1. The USRP gain should be adjusted accordingly so that the amplitude does not exceed 1, but it also should not be too low. Laboratory tests were carried out using an adjustable attenuator in the range from 0 to 110 dB. This allowed to determine in which attenuation range received signal has the maximum available resolution of the converter. The results showed that for the maximum transmitting and receiving gain, the full resolution of the signal amplitude was obtained for attenuation of approximately 80 dB. The transmit power was 20 dBm, and thus the level of the received signal was approx. -60 dBm. For signal levels lower than this value, only part of the available resolution of results is used. The limit value (the noise level) was calculated for attenuation of 120 dB, i.e. the received power of approx. -100 dBm.

4.5.4 Software cooperation

This section describes the flow of data between the AIS system simulator (which is responsible for generating the R-Mode message, correlation and demodulation), and USRP software (which is the interface responsible for controlling USRP devices that perform physical transmission and reception of a radio signal). Figures 4-26 and 4-27 illustrate the data flow between the AIS simulator and the USRP software on the transmitting and receiving side, respectively.

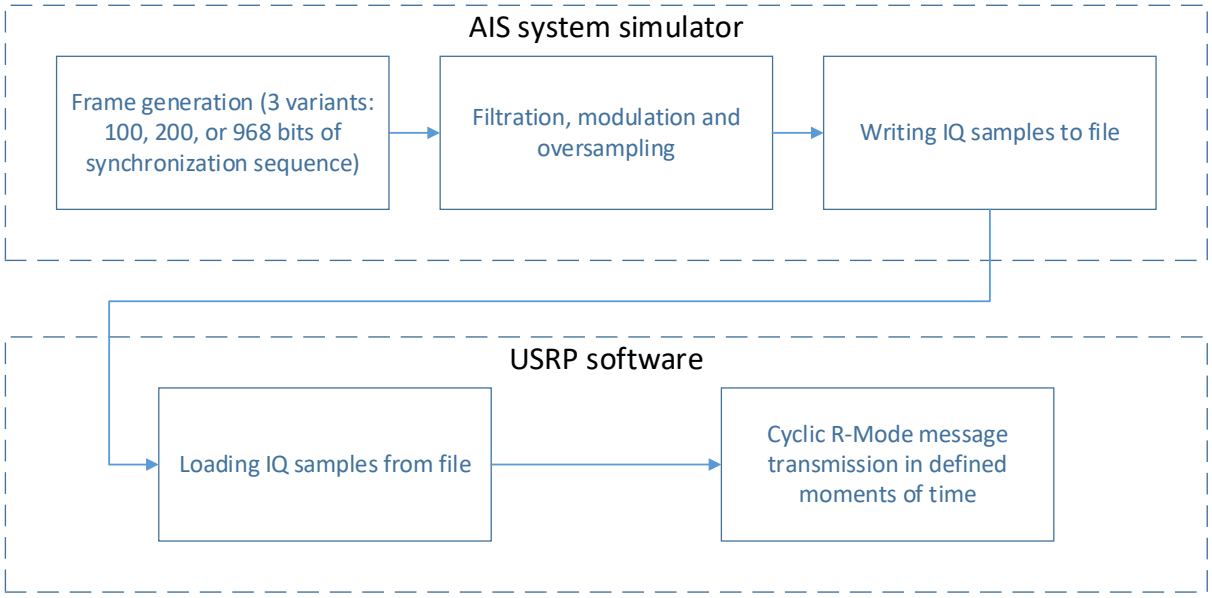

Figure 4-26: Diagram of cooperation between AIS simulator and USRP software on the transmitting side

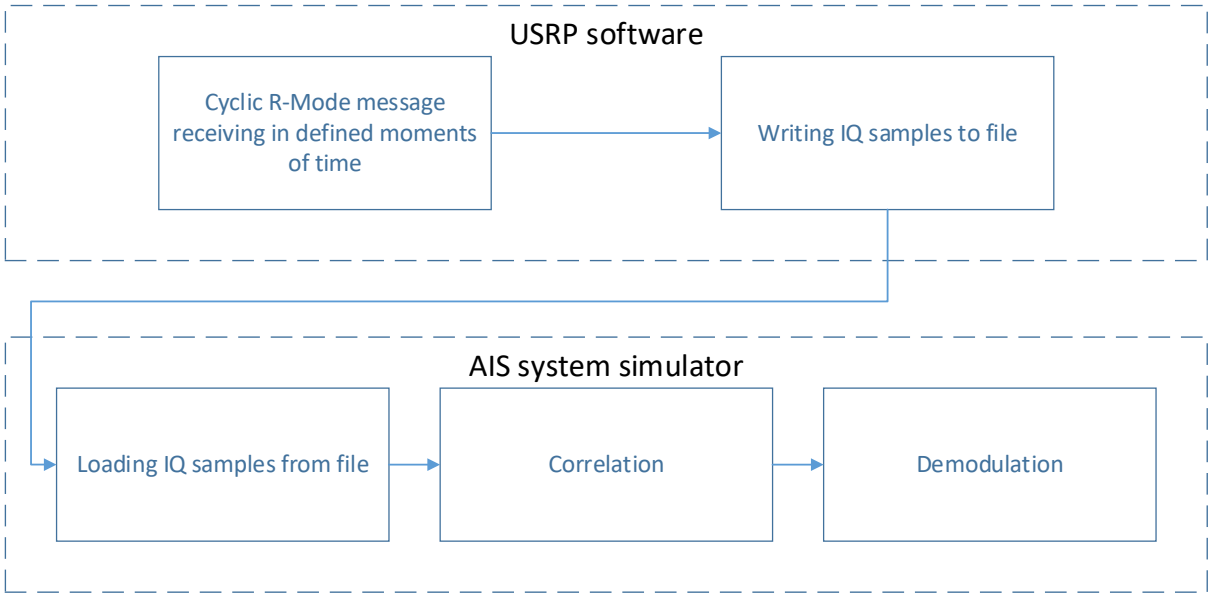

Figure 4-27: Diagram of cooperation between AIS simulator and USRP software on the receiving side

In both cases the interface between the applications are the files with IQ samples (generated or measured). On the receiving side, after the correlation block, the distance between the transmitting and receiving stations is calculated on the basis of the determined transmission delay.

4.5.5 Results of the practical signal transmission test

In the transmission part of the AIS simulator, a packet was generated with an exemplary 200 bit synchronization sequence. The message was subjected to filtration, modulation and oversampling, whereupon the resulting signal in the form of samples I and Q was saved to a file. Next, the signal was read into the USRP platform and was transmitted via a 1 meter cable connected to the second USRP platform and received by it. The received signal was saved and read into the receiving part of the AIS simulator. The signal was then fed to the correlator based on the oversampled signal, where as a result of the correlation with the reference signal, the exact position of the signal could be obtained. The generated correlation function is shown in figure 4-28.

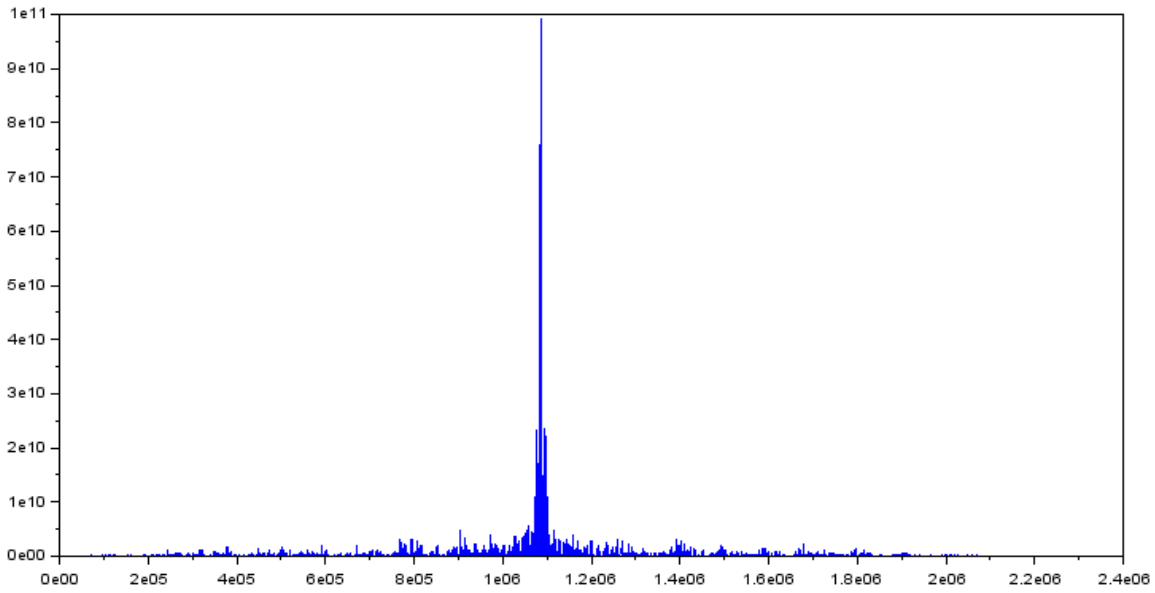

Figure 4-28: Correlation function for practical test

In the laboratory study, a clear correlation peak was obtained, which allowed to determine the exact beginning of the transmitted frame and obtain synchronization for one sample.

5 Measurement methodology

As part of the preparations for the planned measurement campaigns in the Baltic Sea, a measurement stand including a transmission and reception side was designed. In figures 5-1 and 5-2, test-bed transmitter and receiver diagrams was depicted.

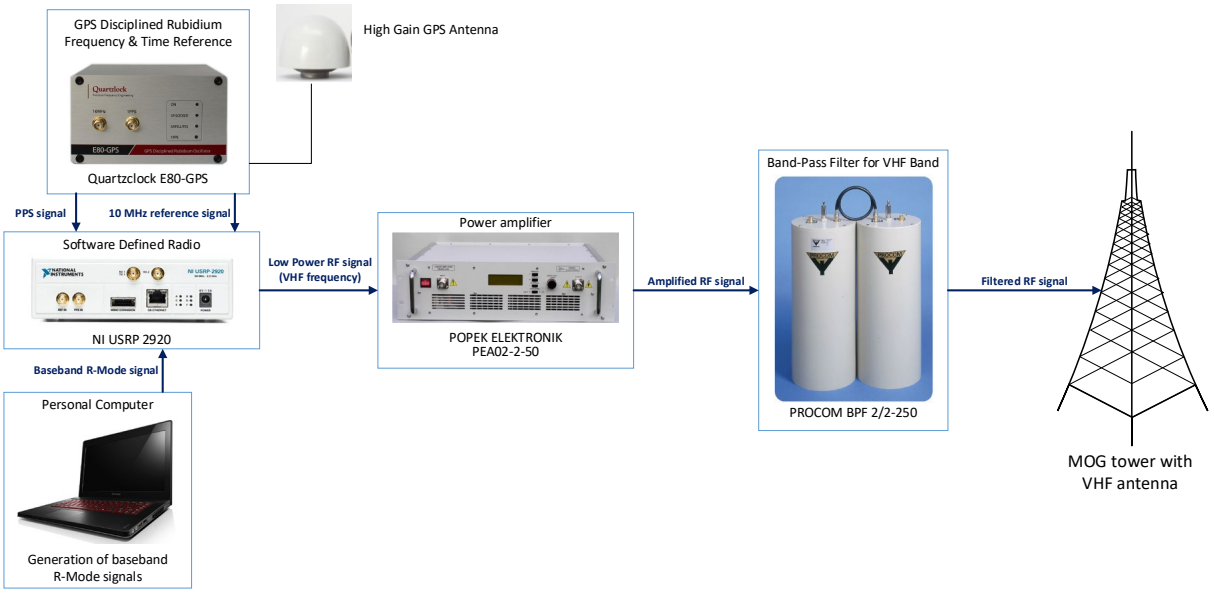

Figure 5-1: Test-bed Transmitter diagram

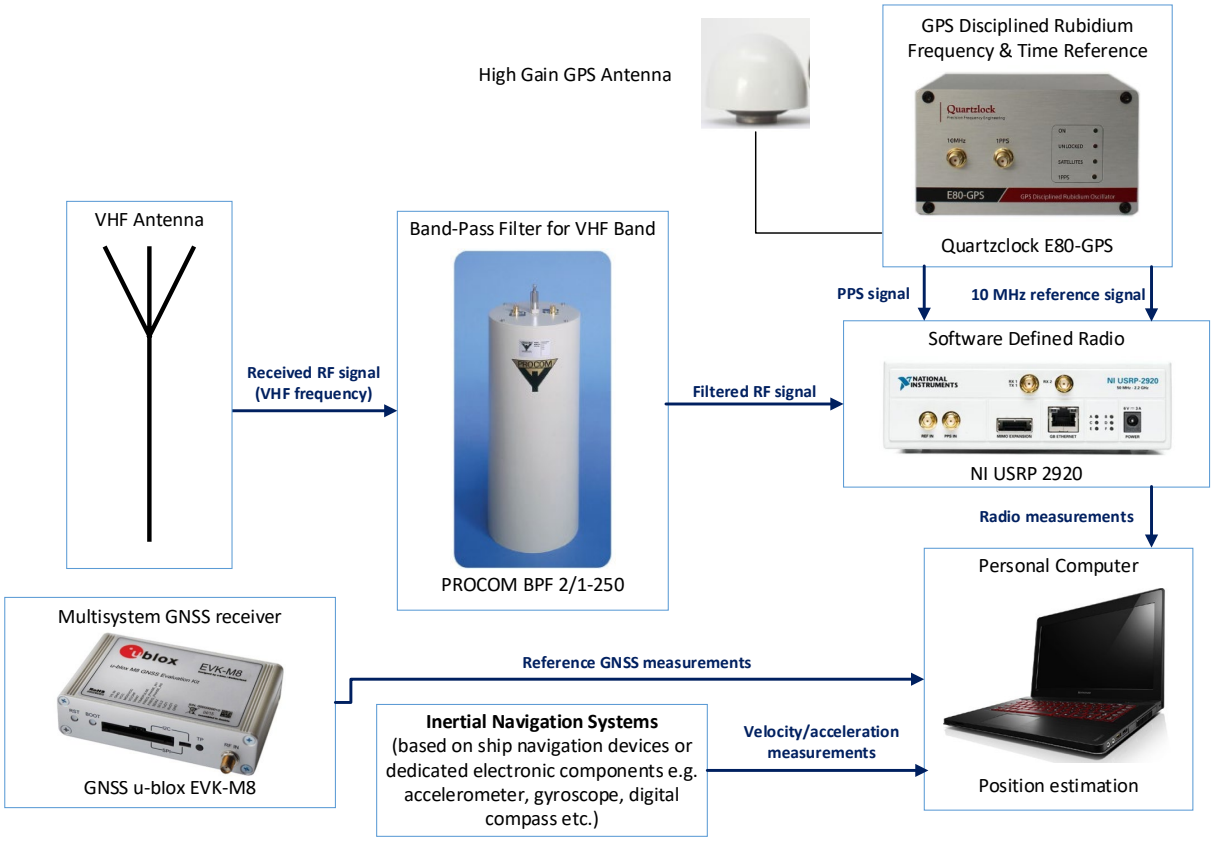

Figure 5-2: Test-bed Receiver diagram

The main elements of the developed measurement system are NI USRP 2920 software defined radios, responsible for transmitting and receiving generated test signals, as well as external rubidium Quartzlock E80 GPS oscillators that provide a stable source of frequency and time (both devices are characterized in detail in chapter 4). This is particularly important for ongoing studies involving the measurement of radio signal propagation time. External oscillators are also used to synchronize the transmitter and receiver part of the system, which will allow to examine the influence of the propagation environment on the distance measurements. In addition to these elements, the measuring sites consist of appropriate bandpass filters, a power amplifier and antennas.

Several stages of measurements have been planned:

- Terrestrial static tests in Gdańsk,
- Onshore static/dynamic tests in Hel (on the Hel Peninsula),
- Marine dynamic measurements on the Bay of Gdańsk,
- Results will be passed to Main R-Mode Sea Trial.

The first test measurement campaign at sea is planned for the spring of 2019, and the measurements will be carried out in cooperation with the Maritime Office in Gdynia (MOG). The MOG will make its VHF antenna installation available for the purpose of the research - to install the transmitter of R-Mode test-bed. It is located on the tower near the entrance to the port in Gdynia. The aim of the measurements is to test, in real conditions, designed signals that will allow to determine the distance between the terminal at sea and the base station on the shore.

During the tests, it is planned to use 4 neighboring channels with a width of 25 kHz each (channels No. 2024, 2084, 2025, 2085 with center frequencies from 161.800 MHz to 161.875 MHz) provided for the VDES [4-4] system (VHF Data Exchange System). NIT obtained a temporary permit from the President of Polish Office of Electronic Communications (Decision No. DZC.WML.5101.3255.2018.2) to use the above-mentioned radio channels for testing the R-Mode system in the area of the Bay of Gdańsk and the Polish territorial waters of the Baltic Sea.

The table 5-1 contains the most important technical parameters of the R-Mode test station, whereas in table 5-2 the receiver technical parameters are presented

Table 5-1: Technical parameters of the R-Mode test station

Location	N 54° 31' 45,36" E 18° 33' 34,48"
Height of the antenna	28 m a.s.l.
Frequency of the transmitter	161.8375 MHz
Antenna type	Radmor 32812/1
Antenna radiation pattern	Omni-directional antenna
Antenna gain	2.15 dBi
Cable attenuation	8.5 dB
ERP power	14.8 dBW
Transmitting device	• National Instruments USRP 2920 • Power amplifier POPEK ELEKTRONIK PEA02-2-50 • Baseband filter PROFCOM BPF 2/2-250
Modulation used	• GMSK (according to ITU-R M.1371-5) • Pi/4-QPSK (according to ITU-R M.2092)

Table 5-2: Technical parameters of the R-Mode test receiver

Sensitivity	-107 dBm
The minimum value of the useful field strength	14 dBμV/m
The maximum value of the interference field strength	12 dBμV/m
Height of the antenna	4 m a.s.l.

On the basis of the assumed parameters, the useful range was determined in accordance with the ITU-R propagation model P.1546-5 [5-1] for various lengths of AIS 26 message. The results are shown in figure 5-3.

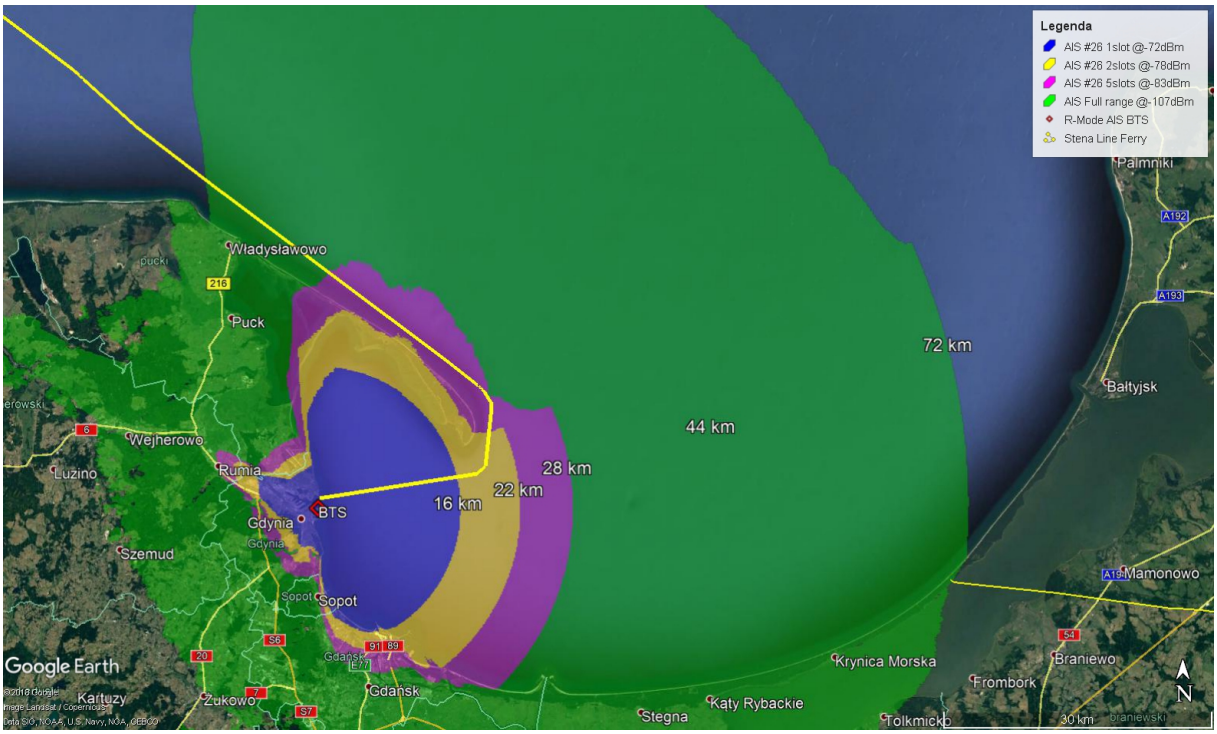

Figure 5-3: Radio planning results for the R-Mode test station in Gdynia

The receiving station will be installed on the Stena Line ferryboat running between Gdynia and Karlskrona. This solution will allow to obtain diversified results (for different distances between the transmitter and the receiver) without the need to rent a vessel, which will reduce the costs of the entire operation. Additionally, the measurement results will be recorded each time for a situation when the vessel moves away from the R-Mode station and when it approaches it. Figure 5-4 presents Stena Line Gdynia-Karlskrona route.

Figure 5-4: Stena Line Gdynia-Karlskrona route

An important element of the measurements will be the logging of the vessel position determined using the GNSS receiver. The fixed position will be converted to the distance to the transmitting station and will be the reference value for the collected measurement values. It will allow to determine the final ranging accuracy of the R-Mode test-bed. For this purpose the GNSS u-blox EVK-M8 (multisystem GNSS + EGNOS receiver) will be used and it will register the most important parameters such as: UTC time, coordinates, velocity, course, and DOP values.

6 Simulator of localization

The main task of the localization simulator is the accuracy prediction of the designed system. Forecasting of the position quality in varied conditions is an important issue in terms of safety. The major factors that contribute to the positioning accuracy deterioration are poor stability of the clocks and reference signal strength decrease.

6.1 Simulator features

The presented simulator is designed for R-Mode project specific requirements. It is developed in such a way that particular modules can be replaced if necessary.

Features provided by simulator:

- TOA based localization,
- Computing value of user clock bias,
- Possibility of TDOA based localization,
- Simulation of errors' sources,
- Calculating HDOP value and other DOP parameters if needed,
- Computing accuracy and precision of localization,
- Calculating RMS and MSE,
- Accuracy improvement by Kalman filtering.

In figure 6-1, the difference between accuracy and precision of position estimation is explained.

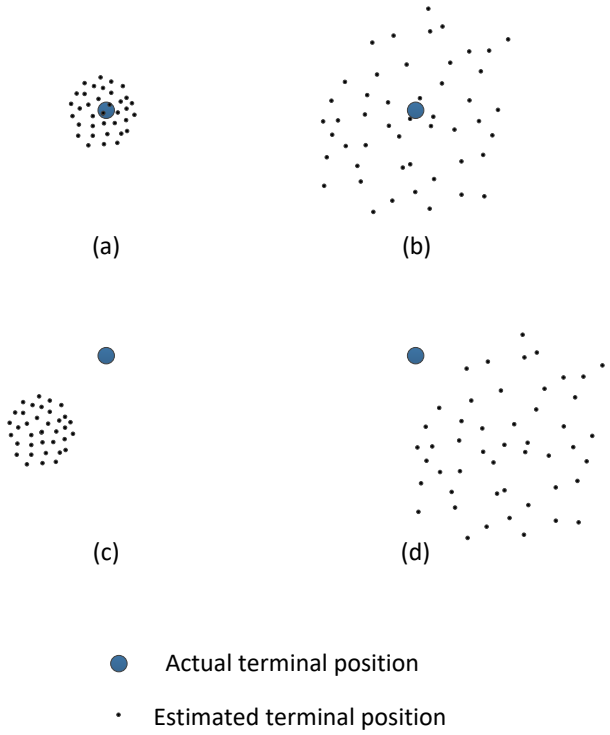

Figure 6-1: Dependence between accuracy and precision of estimation: a) good accuracy and good precision, b) good accuracy and weak precision, c) weak accuracy and good precision, d) weak accuracy and weak precision.

Sources of errors:

- Offsets and drifts of base stations clocks,
- Offset and drift of user terminal clock,
- Decline of accuracy with signal strength decrease as the distance to base station increases,
- Influence of propagation in maritime environment,
- Base stations distribution geometry.

6.2 Simulator description

The localization simulator is based on Time of Arrival (TOA) method. As mentioned, it is possible to replace the TOA algorithm by the Time Difference of Arrival (TDOA) localization method. The terminal's estimated position is computed based on coordinates of reference stations and simulated propagation times of the reference signal. Measurements are software generated and weighted by errors with defined statistical parameters. The magnitude of these errors depends on a chosen scenario and defined conditions. Due to actual terminal position knowledge it is possible to calculate the estimation error. In figure 6-2, the simulator block diagram is shown.

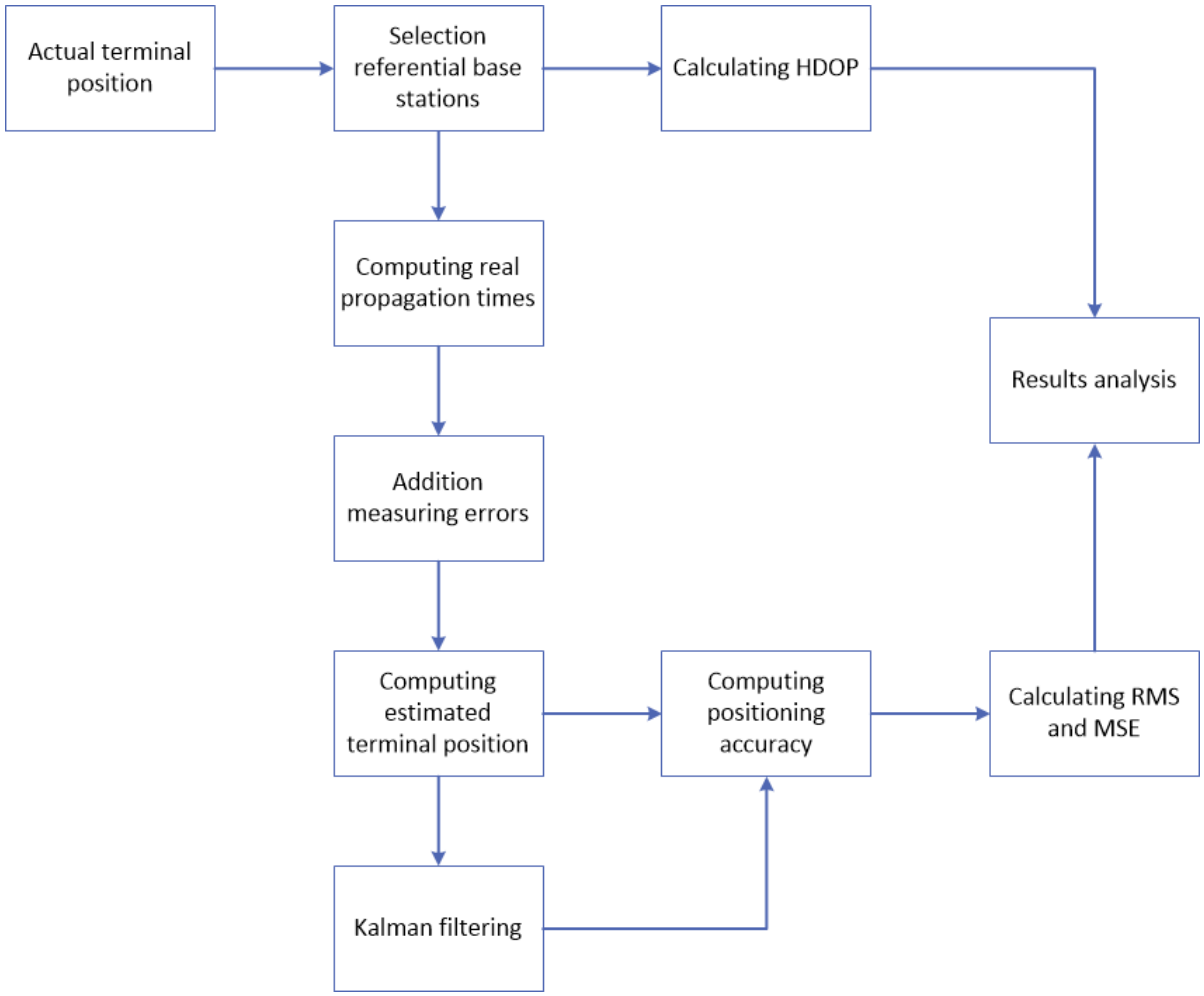

Figure 6-2: Simulator block diagram

Actual terminal position and reference stations coordinates are inputs. Based on them the theoretical value of Horizontal Dilution of Precision is calculated. In order to calculate real propagation times between each reference station and terminal it is necessary to know the real distance taking into account the Earth curvature. It is accomplished by using the WGS84 geodetic system. Real propagation times are calculated as real distance divided by the speed of light. In the next step, the simulated time errors are added.

Time errors are assigned depending on the scenario conditions. Errors consist of components coming from many sources. To each real propagation time components generated by base station and terminal clocks are added. Each clock introduces an error which varies in time and is determined by its drift and offset momentary values. The second significant source of errors is the decline of signal strength as the distance between station and terminal increases.

The estimated terminal position is computed based on the TOA method. To improve the accuracy, user clock bias is calculated and considered. Position estimation error is computed as the distance between the estimated and actual terminal positions, including the Earth curvature.

After multiple determinations of the terminal position for a given simulation scenario, it is possible to perform a statistical error analysis. Mean square error and root mean square error are calculated.

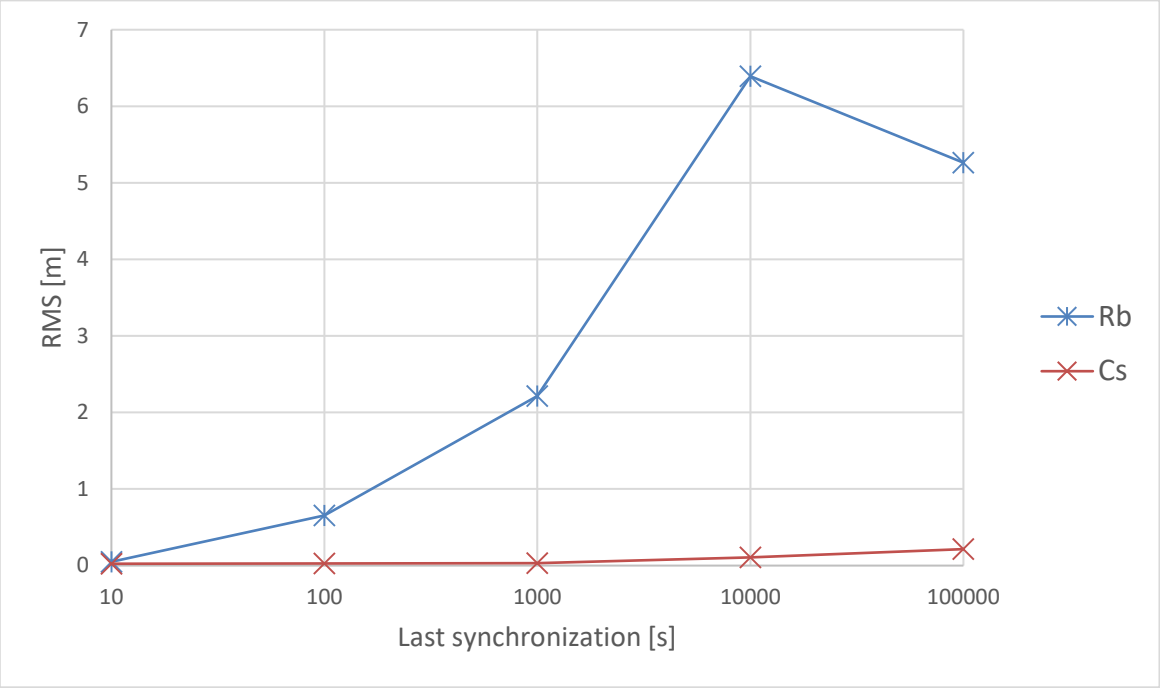

Figure 6-3: Root mean square estimation error in dependence of lost synchronization time and reference stations clocks (Rubidium and Cesium)

Kalman filtering block is designed to improve accuracy in dynamic scenarios. The Kalman filter's input values are from the radio navigation system and inertial navigation system. Position estimation based on radio measurements is corrected by results of velocity (speed and course) measurements. The scheme of Kalman filtering block is shown in figure 6-4.

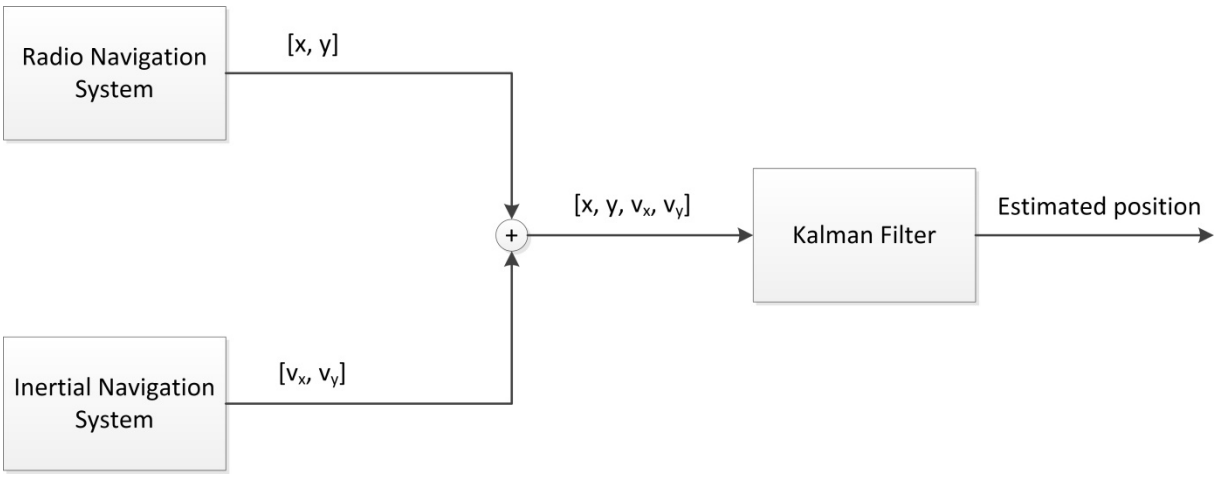

Figure 6-4: Block diagram of Kalman filter usage

6.3 Example simulation

In figure 6-5, the actual target position (orange) and reference stations positions (red) are shown.

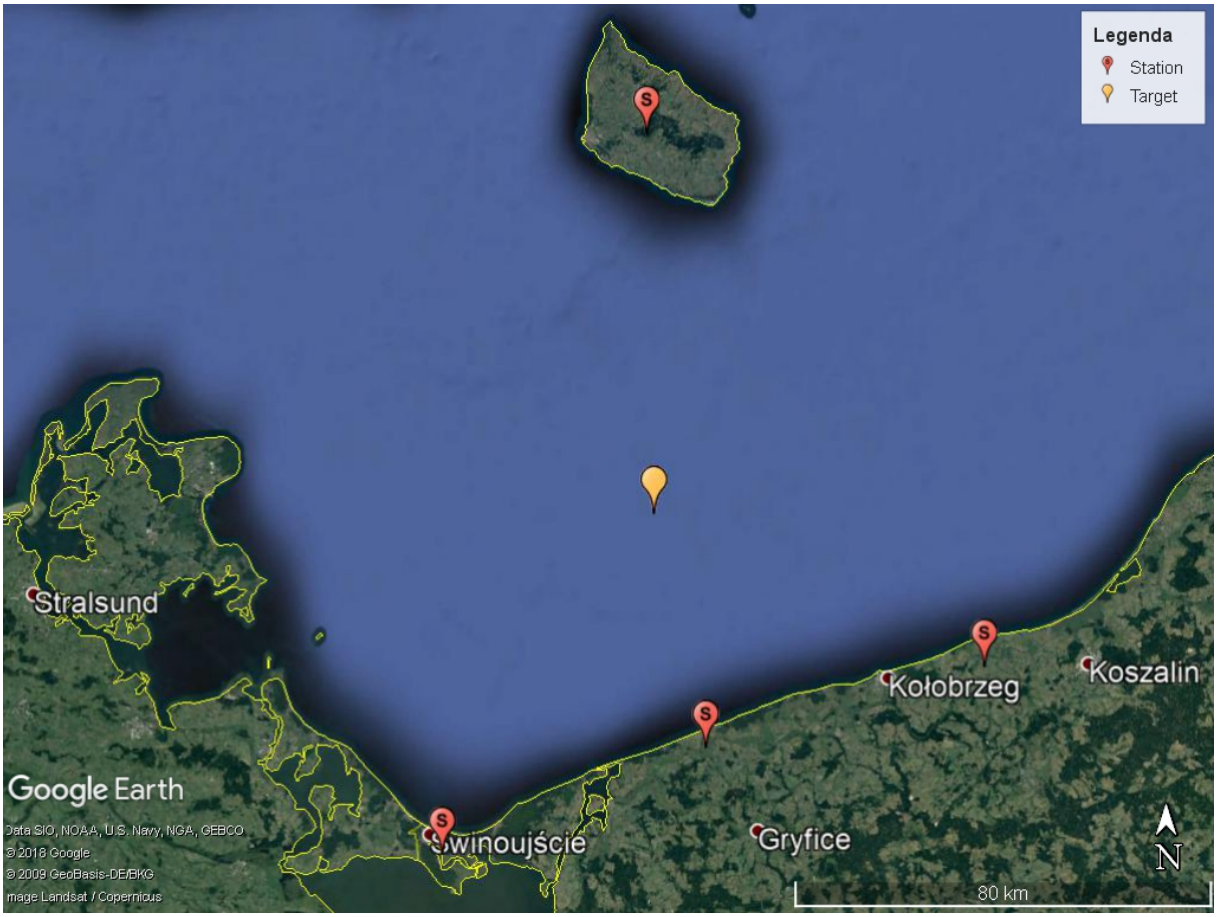

Figure 6-5: Geometry of reference stations and terminal

In figure 6-6, the example results of static scenario simulation are presented. In that scenario the target and stations geometry above was used. In part a) of the figure, the estimation result 1000 seconds after synchronization loss is presented. In part b) of the figure, the estimation result 10000 seconds after synchronization loss is shown.

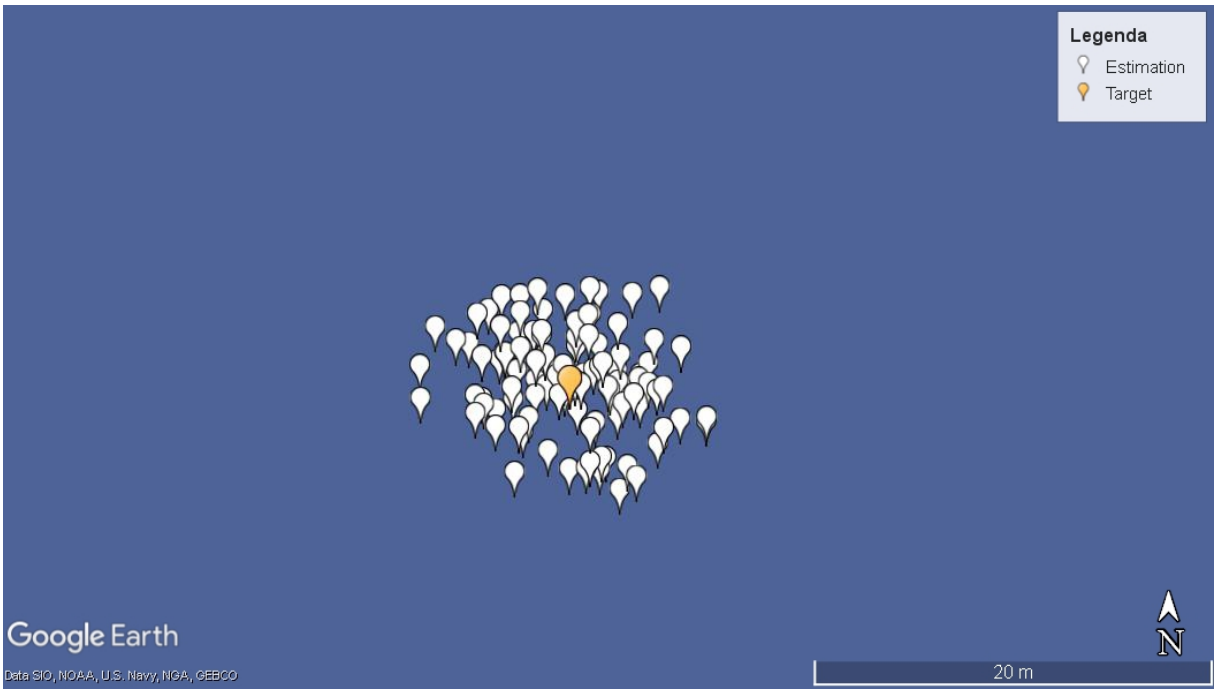

(a)

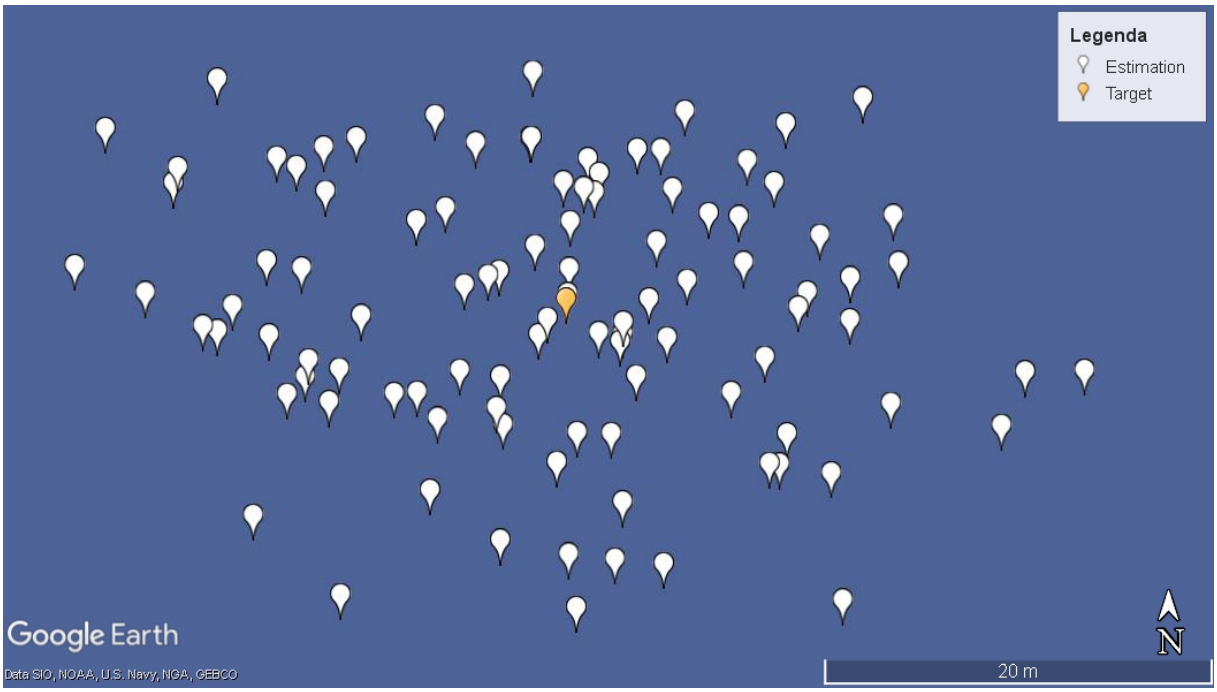

{b}

Figure 6-6: Sample results of static scenario simulation: a) estimation result 1000 seconds after synchronization loss, b) estimation result 10000 seconds after synchronization loss

7 Phenomena occurring in the troposphere

7.1 General information

This chapter will address the following aspects relevant to radio wave propagation in the VHF Band:

- The troposphere and its phenomena that affect the operation in the VHF Band
- Major phenomena the impact the AIS signals
- Modeling and estimation of the delay value

In the troposphere, i.e. the lowest layer of Earth's atmosphere, one can distinguish the following phenomena which affect the VHF Band signal propagation [7-1]:

- Diffraction
- Tropospheric scattering
- Meteoric bursts
- Sporadic propagation of the ionospheric E layer
- Atmospheric ducting
- Rain scatter
- Radiowave reflection and refraction

Given the above, the following effects are the most critical with respect to the range and quality of the AIS signal [7-2]:

- Diffraction over the sea around the curvature of the Earth
- Atmospheric ducting
- Multipath effects

Some of the phenomena mentioned above have long-term effect on the interference characteristics, whereas the other are much more instantaneous (short-term) in nature. This observation is reflected in figures 7-1 and 7-2.

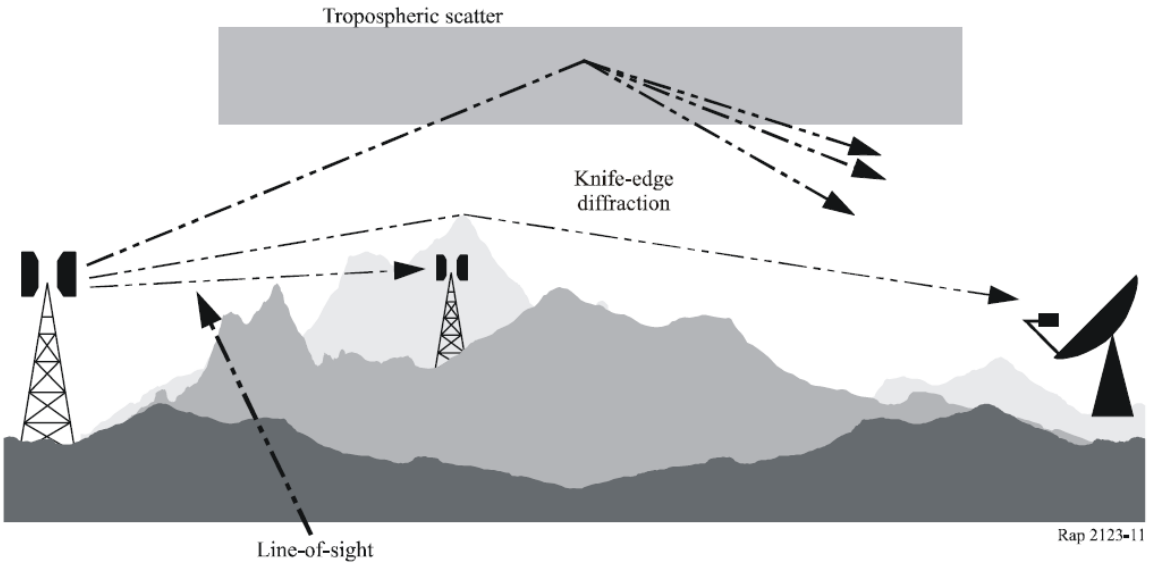

Figure 7-1: Propagation mechanisms with a long-term effect on the interference characteristics [7-1]

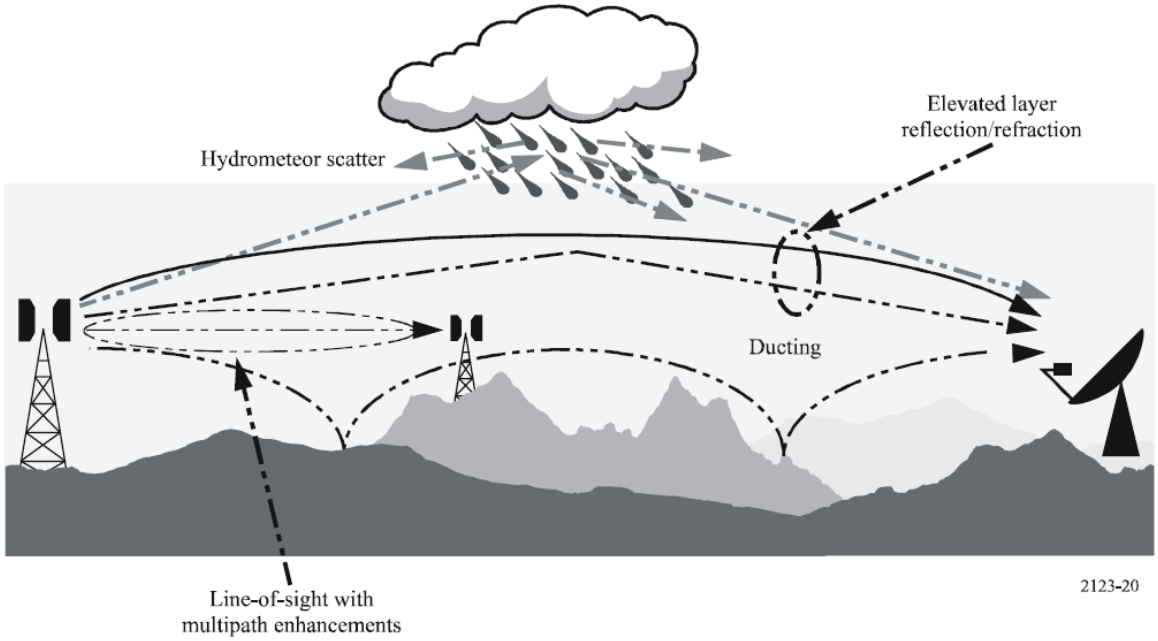

Figure 7-2: Propagation mechanisms with a short-term effect on the interference characteristics [7-1]

Similarly to the typical VHF terrestrial systems, the maximum range of the AIS system can be achieved in the line-of-sight (LOS) conditions and using the diffraction mode propagation mechanism. There is a number of factors that impact the latter, including: frequency, distance, transmitting/receiving antenna height, surface conductivity and admittance, polarization. That being said, it has to be underlined that the last three factors are generally insignificant as far as the AIS is concerned [7-1].

There is a number of ITU-R documents that discuss the diffraction effects:

- Recommendation ITU-R P.526 which analyses the field strength at the receiving station [7-3]
- Recommendation ITU-R P.452 which analyses numerous effects (including diffraction) as sources of interference between stations on the Earth's surface [7-4]
- Recommendation ITU-R P.1406 which discusses the influence of various effects (including diffraction) on the channel characteristics. One of such effects is delay spread which is crucial for digital systems operating in multipath environment [7-5]
- Recommendation ITU-R P.1407 which discusses multipath environment and defines parameters necessary for its statistical description [7-6]

As stated in [7-6], the multipath mobile channel can be characterized in terms of its impulse response which varies at a rate dependent on the speed of the mobile and/or the scatterers. Consequently, the characteristics of the mobile radio channels can be expressed by:

- The power delay profiles
- The Doppler spectra

and both these parameters can be obtained from wideband channel sounding measurements (after appropriate signal processing).

The recommendation [7-6] distinguishes channel parameters with respect to their "scale". Statistics of small-scale parameters are used to produce cumulative distribution functions (CDFs). The medium-scale CDF covers a particular route of measurement, usually in the order of tens to hundreds of meters. After that, the combined data set from a number of medium-scale routes is considered to be a large-scale or global characterization, which is representative of the entire surveyed environment, e.g. hilly terrain, urban, suburban, indoor large rooms, corridors, etc. [7-6].

The required parameters which statistically describe the channel over time can be obtained from three types of power delay profiles:

- Instantaneous power delay profile
- Short-term power delay profile
- Long-term power delay profile

The graphical representation of those can be seen in fig. 7-3.

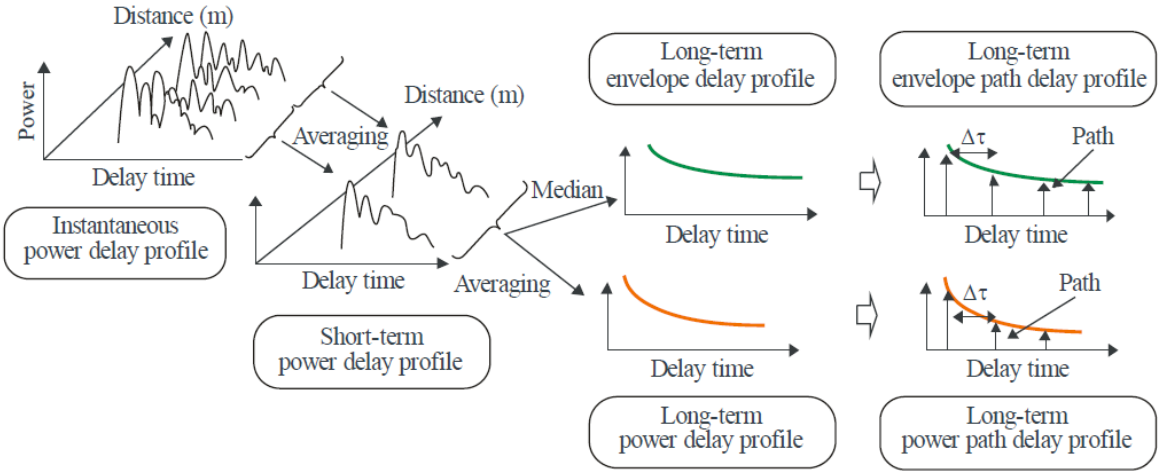

Figure 7-3: Power delay profiles definition [7-6]

Recommendation [7-6] introduces the following definitions:

- The instantaneous power delay profile is the power density of the impulse response at one moment at one point.
- The short-term (small-scale) power delay profile is obtained by spatially averaging the instantaneous power delay profiles over several tens of wavelengths within the range where the same multipath components are maintained in order to suppress the variation of rapid fading.
- The long-term power delay profile is obtained by spatially averaging the short-term power delay profiles at approximately the same distance from the base station (BS) in order to suppress the variations due to shadowing.

Additionally, [7-6] defines a number of statistical parameters of the channel, including the formulas needed to derive their values. That includes:

Total power of the impulse response, pm, defined as:

$$p_m = \int_{t_0}^{t_3} p(t)dt \tag{7.1}$$

Where:

p(t): power density of the impulse response in linear units of power

t: delay with respect to a time reference

t_0: instant when $p(t)$ exceeds the cut-off level for the first time

t_3: instant when $p(t)$ exceeds the cut-off level for the last time [7-6].

Average delay time ,T_D, is the power weighted-average of the excess delays measured which is given by the first moment of the power delay profile, i.e.:

$$T_D = \frac{\int_0^{\tau_e} \tau p(\tau)d\tau}{\int_0^{\tau_e} p(\tau)d\tau} - \tau_a \tag{7.2a}$$

where:

τ: excess time delay variable and is equal to $t - t_0$

τ_a: arrival time of the first received multipath component (first peak in the profile)

τ_e: $t_3 - t_0$

In discrete form with time resolution $\Delta\tau$ (= 1/*B*), equation (7.2a) becomes:

$$T_D = \frac{\sum_{i=1}^{N} \tau_i p(\tau_i)}{\sum_{i=1}^{N} p(\tau_i)} - \tau_M \tag{7.2b}$$

$$\tau_i = (i-1)\ \ \Delta\tau = \frac{\mathrm{i}-1}{\mathrm{B}} \qquad (i = 1,2,\dots,N)$$

where i = 1 and N are the indices of the first and the last samples of the delay profile above the threshold level, respectively, and M is the index of the first received multipath component (first peak in the profile)

The delays may be calculated using the following relationship:

$$t_i(\mu s) = 3.3 r_i\ [km] \tag{7.3}$$

where r_i is the sum of the distances from the transmitter to the multipath reflector, and from the reflector to the receiver, or is the total distance from the transmitter to receiver for t_{LOS} [7-6].

The rms delay spread [6], S, is the power weighted standard deviation of the excess delays and is given by the second moment of the power delay profile. It provides a measure of the variability of the mean delay. In numerical form, this parameter can be expressed as follows:

$$S = \sqrt{\frac{\int_0^{\tau_e} (\tau - T_D - \tau_a)^2 p(\tau) d\tau}{\int_0^{\tau_e} p(\tau) d\tau}} \tag{7.4a}$$

In discrete form with time resolution Δτ, equation (4a) becomes:

$$S = \sqrt{\frac{\sum_{i=1}^{N} (\tau_i - T_D - \tau_M)^2 p(\tau_i)}{\sum_{i=1}^{N} p(\tau_i)}} \tag{7.4b}$$

Delay window [7-6], W_q: the length of the middle portion of the power delay profile containing a certain percentage, q, (typically 90%) of the total power found in that impulse response. In numerical form, this parameter can be expressed as follows:

$$W_q = (t_2 - t_1) \tag{7.5}$$

whereby the boundaries t_1 and t_2 are defined by:

$$\int_{t_1}^{t_2} p(t) dt = \frac{q}{100} \int_{t_0}^{t_3} p(t) dt = \frac{q}{100} p_m \tag{7.6}$$

and the power outside of the window is split into two equal parts $\left(\frac{100-q}{200}\right) p_m$.

The delay interval [7-6], I_{th}, is defined as the time difference between the instant t_4 when the amplitude of the power delay profile first exceeds a given threshold P_{th}, and the instant t_5 when it falls below that threshold for the last time:

$$I_{th} = (t_5 - t_4) \tag{7.7}$$

The number of multipath or signal components can be represented from the delay profile as the number of peaks whose amplitudes are within *A* dB of the highest peak and above the noise floor [7-6].

To provide more in-depth explanation of the above parameters, figure 7-4 below might prove helpful.

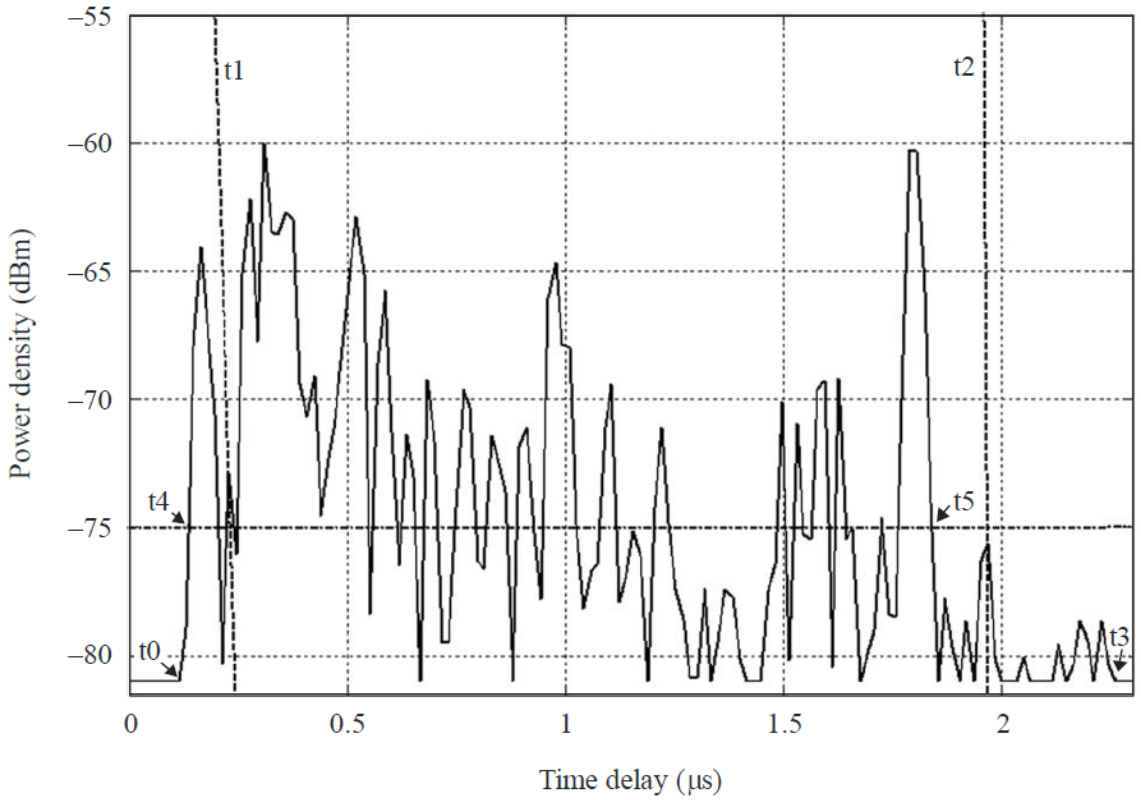

Figure 7-4: Power delay profile [7-6]

Fig. 7-4 illustrates the following parameters: the delay window, W_{90}, containing 90% of the received power is marked between the two vertical dashed lines (t_1 and t_2), the delay interval, I_{15}, containing the signal above the level 15 dB below the peak, lies between t_4 and t_5. t_0 and t_3 indicate the start and the end of the profile above the noise floor.

The parameters defined in recommendation [7-6] can be measured using sounding signals. After that they can be used:

- To determine power delay profile and other relevant delay parameters,
- To model the channel as a tapped delay line.

In case of this work, the delay parameters can be obtained from the instantaneous power delay profile and the synchronization signals could be used for the purposes of sounding.

7.2 A practical example of using the CIR method (channel impulse response)

In the following example – which is based on article [7-7] – the measurement of radio channel impulse response was presented for the cases of sea and coastal areas. The system under analysis was operating using the 1457 MHz frequency with the 10 MHz band and the OFDM technique. In the paper, the power spread profile was determined, alongside the rms value of the delay spread.

During the analysis, a BPSK wave modulated by a pseudorandom binary sequence, PRBS-16, was used as a sounding signal. The parameters of that wave are listed below:

- Bit rate: 5 Mb/s

- Repetition period: 13.107 ms
- Width of the spectrum main lobe: 10 MHz
- Center frequency: 1457 MHz
- Transmitted signal power: 10 W.

The sounding signal was transmitted from a single, fixed point located at the Hel Peninsula, whereas the received signal was recorded at two mobile stations: aboard the plane and aboard the boat. Fig. 7-5 indicates the transmitter's location and the routes the mobile stations. The signal was recorded in the form of binary files containing the I/Q samples in the baseband with a duration of 5 seconds. Additionally, text files were recorded which contained time and location markers obtained via an independent GPS receiver. The vector signal generator SMU 200A (by Rohde&Schwarz) with a power amplifier was employed as the transmitter. On the other hand, the receiver was comprised of a bandpass filter with a SDR platform (USRP 2920) and a PC to control the receiver operation and to record/store the signals.

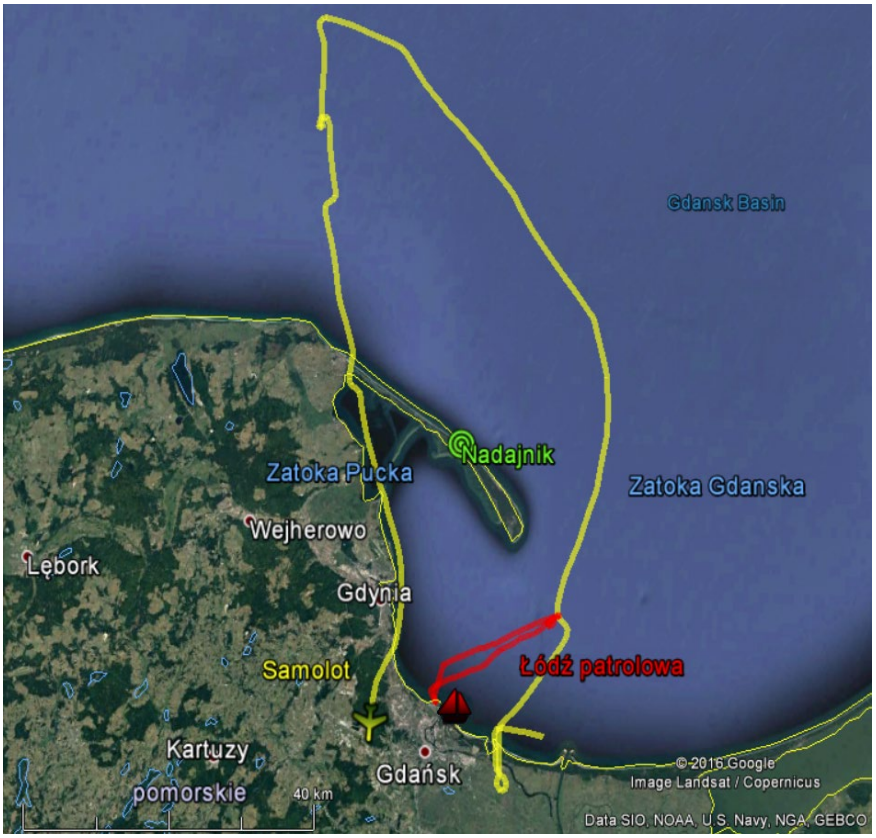

Figure 7-5: Location of the transmitter (green point in the picture) and the routes of mobile platforms (plane – yellow line, boat – red line) [7-7]

After the initial processing of the recorded data (synchronization of the signal with the PRBS-16 sequence and the Doppler effect removal), the module of the channel impulse response $|h(\tau)|$ was obtained. After that, the power delay profile, PDP, was derived using the formula:

$$P(\tau) = \sum_{i=1}^{M} |h(t_i, \tau)|^2 \tag{7.8}$$

A sample PDP is presented in fig. 7-6.

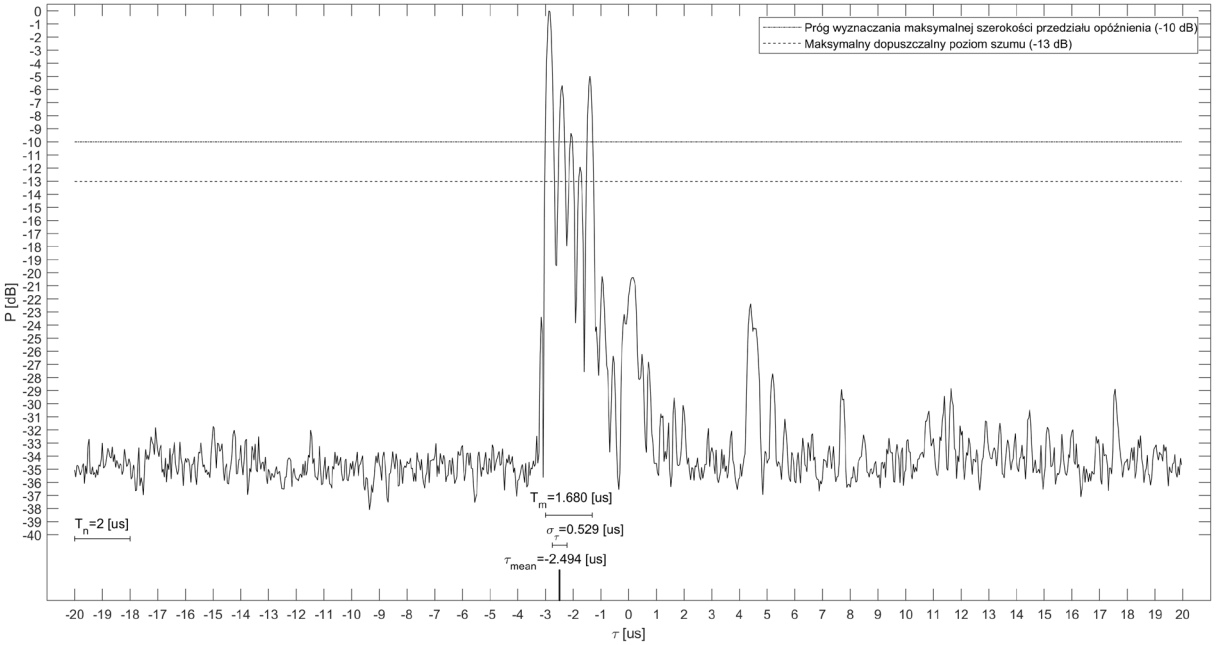

Figure 7-6: Power delay profile (example). Solid horizontal line denotes a threshold for the determination of the maximum delay range width (-10 dB), dotted horizontal line represents the maximum acceptable noise level (-13 dB) [7-7]

In the next step, the mean excess delay was calculated, using the following formula:

$$\tau_{mean} = \frac{\int_{\tau_{min}}^{\tau_{min}+T_M} \tau P(\tau) d\tau}{\int_{\tau_{min}}^{\tau_{min}+T_M} P(\tau) d\tau} \tag{7.9}$$

Subsequently, the rms delay spread was obtained with the following expression:

$$\sigma_{tau} = \sqrt{\frac{\int_{\tau_{min}}^{\tau_{min}+T_M} (\tau-\tau_{mean})^2 \cdot P(\tau) d\tau}{\int_{\tau_{min}}^{\tau_{min}+T_M} P(\tau) d\tau}} \tag{7.10}$$

Additionally, a histograms of the rms delay spread and the CDFs (cumulative distribution function) were calculated for the signals received in the plane and in the boat (at high seas and in the vicinity of the port). Fig. 7-7 and 7-8 show these characteristics for the boat (in the vicinity of the port).

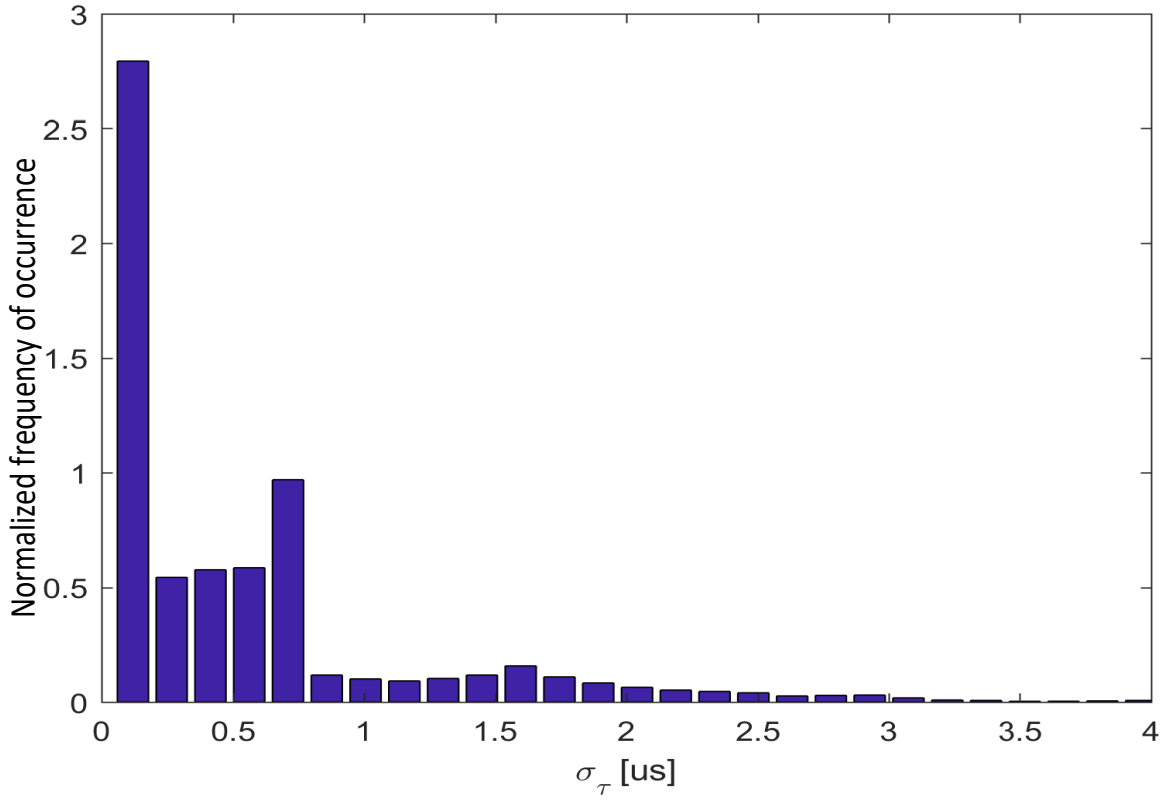

Figure 7-7: RMS delay spread histogram (signal recorded aboard the boat – vicinity of the port) [7-7]

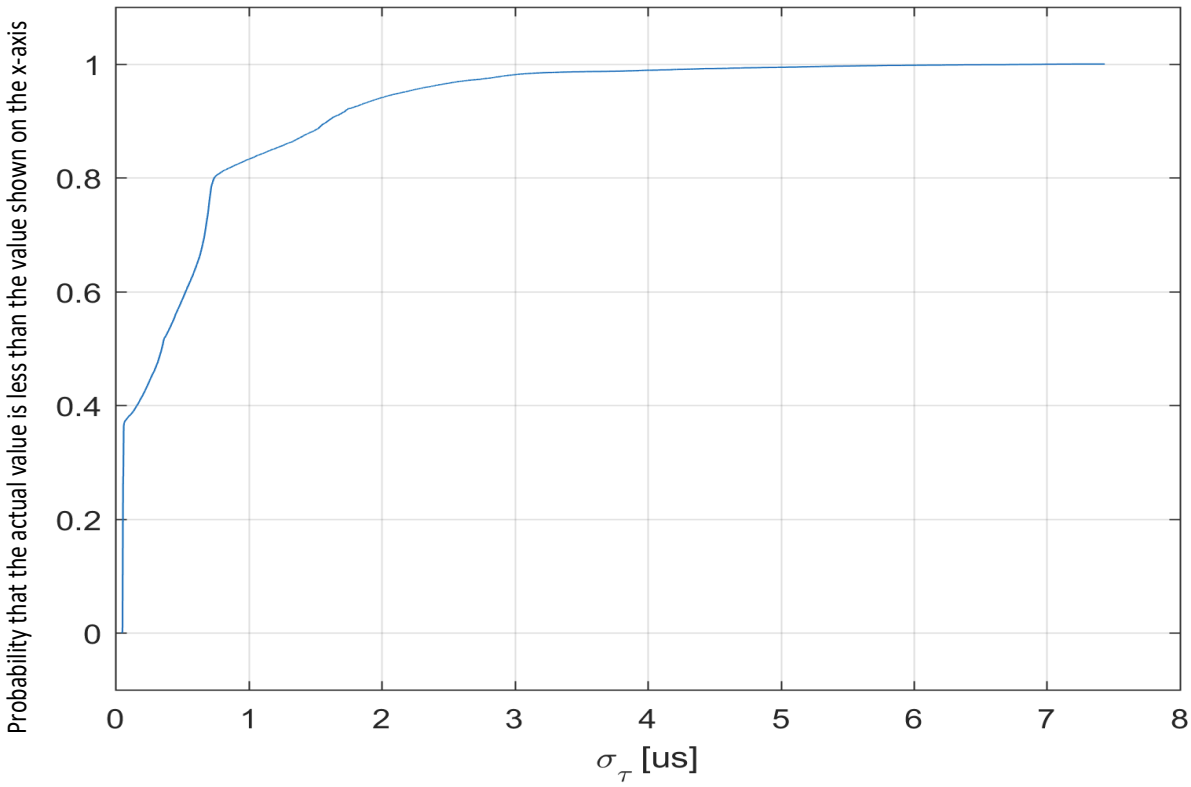

Figure 7-8: CDF for the signal recorded aboard the boat – vicinity of the port [7-7]

The selected statistical values of the rms delay spread obtained for the three analyzed scenarios are presented in table 7-1.

Table 7-1: Statistical values of the rms delay spread obtained in article [7-7]

	Plane [μs]	Boat, high seas [μs]	Boat, around the port [μs]
Minimum	0,047	0,046	0,046
Mean	0,066	0,058	0,597
Maximum	8,459	0,254	7,434

From the above data, it is clearly visible that propagation conditions were favorable in the cases of the plane and the boat at high seas, while they were significantly worse in case of the boat in the vicinity of the port.

To sum up: the presented method of the wideband channel analysis can be successfully employed for the statistical parameters estimation of such channels.

8 Summary

The activities conducted by the National Institute of Telecommunications in the R-Mode GAs 5.3 and 5.4 (and described in this report) were mostly conceptual and simulation work. Now, the results obtained up to this point need to be confirmed in the target environment (i.e. at sea).

For spring 2019, a wide measurement campaign is planned whose goal is to confirm the feasibility of the AIS-based solutions for the purposed of the planned R-Mode system. The campaign will be divided into three stages:

- Terrestrial and static tests in Gdańsk
- Onshore static/dynamic tests in Hel (on the Hel Peninsula)
- Dynamic measurements at the Baltic Sea (within the Bay of Gdansk area) which will be conducted using the Stena Line ferry travelling between Gdynia and Karlskrona. A several repetitions of this campaign are anticipated to obtain more reliable results.

As explained in the report, the vast majority of the preparations for the campaign is already completed, and some minor remaining organizational issues are being handled now.

The results that will be obtained during the campaign (alongside the software developed by the NIT) will serve a major contribution into the main R-Mode sea trial coordinated by other project partners.

9 References

[2-1] R-Mode Baltic - Baseline and Priorities

[2-2] Recommendation ITU-R M.1371-5 (02/2014), *Technical characteristics for an automatic identification system using time division multiple access in the VHF maritime mobile frequency band*

[2-3] 3GPP TS 25.213 V15.0.0, 2018, “Technical Specification Group Radio Access Network; Spreading and modulation (FDD)”.

[3-1] ITU-R P.1546-5, 2013, “Method for point-to-area predictions for terrestrial services in the frequency range 30 MHz to 3 000 MHz”

[4-1] ITU-R M.1371-5, 2014,“Technical characteristics for an automatic identification system using time division multiple access in the VHF maritime mobile frequency band”.

[4-2] National Instruments, 2012, “NI USRP™-2920 Specifications: 50 MHz to 2.2 GHz Tunable RF Transceiver”.

[4-3] Quartzlock E80-GPS Specification: GPS Disciplined Rubidium Frequency & Time Reference

[4-4] ITU-R M.2092-0, 2015, "Technical characteristics for a VHF data exchange system in the VHF maritime mobile band".

[5-1] ITU-R P.1546-5, 2013, “Method for point-to-area predictions for terrestrial services in the frequency range 30 MHz to 3 000 MHz”.

[7-1] Report ITU-R M.2123-2007; Long range detection of automatic identification system (AIS) messages under various tropospheric propagation conditions

[7-2] D. Green et al.; „VHF Propagation Study”, 2011

[7-3] Rec. ITU-R P.526-14 (01/2018); Propagation by diffraction

[7-4] Rec. ITU-R P.452-16 (07/2015); Prediction procedure for the evaluation of interference between stations on the surface of the Earth at frequencies above about 0.1 GHz

[7-5] Rec. ITU-R P.1406-2 (07/2015); Propagation effects relating to terrestrial land mobile and broadcasting services in the VHF and UHF bands

[7-6] Rec. ITU-R P.1407-6 (06/20170; Multipath propagation and parameterization of its characteristics

[7-7] Jędrzej Hajduczenia „Pomiar odpowiedzi impulsowej kanału radiowego na obszarze morskim i przybrzeżnym”, KSTiT 2017 (article in Polish)